UNIVERSITÀ
DI PAVIA

Dipartimento di Biologia e Biotecnologie "L. Spallanzani"

Master's degree in Neurobiology

Modelling α-synuclein pathology in experimental ischemic stroke

Studio della patologia da α-sinucleina in modelli sperimentali di ictus ischemico

Relatore:
Dr. Marco Peviani

Correlatore:
Dott.ssa Tizibt Ashine Bogale

Tesi Sperimentale di
Paolo Treccani

Anno Accademico 2023/2024

ITALIAN ABSTRACT

L'ictus continua a rappresentare una delle principali cause di morte e disabilità a livello mondiale, con opzioni terapeutiche ancora limitate. Il danno vascolare e l'infiammazione sono correlati con una maggiore gravità dell'ictus e con esiti clinici peggiori nei pazienti. L'alfa-sinucleina (α-syn), una proteina neuronale ampiamente nota per il suo ruolo patogeno nelle malattie neurodegenerative croniche, come il morbo di Parkinson, è coinvolta anche nel danno cerebrale acuto che segue un ictus ischemico, modulando il danno vascolare e i processi di recupero. In questo studio abbiamo analizzato, in un modello in vivo di ictus ischemico, l'impatto delle forme patologiche dell'α-syn sul danno cerebrale e sul recupero della lesione ischemica nelle sue fasi acute, sub-acute e croniche. Abbiamo inoltre sviluppato un modello in vitro non cellulare di aggregazione dell'α-syn in condizioni che mimano l'ischemia per testare l'effetto di potenziali composti/farmaci terapeutici. Per lo studio in vio, l'ischemia cerebrale focale transitoria è stata indotta in topi wild-type C57BL/6RCC e in topi C57BL/6S con delezione spontanea dell'α-syn mediante occlusione transitoria unilaterale dell'arteria cerebrale media (tMCAo) per 30 minuti. I topi sono stati valutati per i deficit sensorimotori al giorno 9 tramite una scala di valutazione chiamata *neuroscore*, per il fenotipo ansioso e la funzionalità locomotoria generale al giorno 28 tramite EPM (*elevated plus maze*), per l'apprendimento spaziale e la memoria ai gironi 30-35 tramite il test del labirinto di Barnes e per la sopravvivenza fino all'*endpoint* sperimentale. La risonanza magnetica (MRI) è stata utilizzata per analizzare longitudinalmente la dimensione dell'infarto, l'emodinamica e l'edema cerebrale. Abbiamo osservato una maggiore sopravvivenza complessiva nei topi knock-out, nonostante deficit sensorimotori comparabili nella fase sub-acuta della tMCAo. Tuttavia, i topi *knock out* per α-syn hanno mostrato la riduzione del tempo trascorso nella zona centrale dell'apparato EPM, suggerendo un comportamento esplorativo alterato, e un apprendimento compromesso rispetto ai controlli sham nel test del labirinto di Barnes. Questi dati suggeriscono che l'assenza della α-syn endogena predisponga i topi ad una maggiore sensibilità all'ictus ischemico. In linea con questa osservazione, i topi non esprimenti α-syn hanno mostrato lesioni più estese, un deficit nel flusso cerebrovascolare e un edema cerebrale più esteso rispetto ai topi wild-type nell'analisi MRI a 3 giorni dalla tMCAo. Tuttavia, questi topi hanno mostrato un marcato recupero in tutti i parametri a 7 giorni, quando i valori MRI sono tornati simili a quelli misurati nei topi wild type. Questa osservazione suggerisce che esista un effetto temporale legato alla α-syn nella fisiopatologia del danno ischemico. In particolare, mentre le forme monomeriche fisiologiche sono importanti nel supportare le funzioni vascolari, quelle aggregate patologiche, che si formano a seguito dello stimolo ipossico, contribuiscono al danno cerebrovascolare. Per valutare il ruolo distinto della α-syn endogena (monomerica) e di quella tossica (aggregata) sulla vascolatura cerebrale, abbiamo utilizzato un modello in vitro di

ipossia/riossigenazione in cellule endoteliali microvascolari. In breve, le cellule sono state esposte alla α-syn monomerica all'inizio del periodo di ipossia o durante la ripresa della riossigenazione. Abbiamo osservato che la prima condizione, in cui α-syn veniva aggiunta durante l'ipossia, induceva un aumento di *ICAM-1*, un mediatore infiammatorio, da parte delle cellule microvascolari. Al contrario, l'aggiunta di α-syn nel periodo di riossigenazione permetteva una riduzione di *ICAM-1*. Complessivamente, questi dati indicano che esista un effetto tossico della α-syn condizionata dall'ambiente ipossico, e un effetto benefico della sua forma fisiologica. Per caratterizzare meglio l'effetto delle condizioni ipossiche sulle alterazioni strutturali della proteina α-syn e per testare composti in grado di inibire l'aggregazione patologica della proteina, abbiamo inizialmente effettuato l'aggregazione in vitro della α-syn a pH acido per mimare una condizione solo ipossica, seguita da co-aggregazione delle fibrille generate a pH acido con α-syn monomerica a pH fisiologico (condizione di riossigenazione. Abbiamo osservato una struttura compatta a beta-foglietto e una maggiore capacità di "seeding" degli aggregati ischemici rispetto a quelli generati in tampone a pH fisiologico. Abbiamo anche osservato che l'aggregazione dell'α-syn veniva completamente inibita dalla clusterina in condizioni che mimano l'ipossia/riossigenazione e dalla doxiciclina in tampone a pH fisiologico.

Nel complesso, i nostri dati suggeriscono che l'impatto della α-syn sul danno cerebrale o sul recupero dopo ictus ischemico può essere influenzato dalla generazione delle sue specie tossiche a seguito dello stimolo ischemico iniziale. In particolare, durante le fasi sub-acute e croniche della patologia, la generazione delle forme tossiche di α-syn, causata dall'ambiente ipossico in cui la proteina si trova, potrebbe essere dannosa e compromettere il rimodellamento cerebrale. La disponibilità di modelli sperimentali in grado di analizzare e riprodurre questi cambiamenti dinamici della α-syn e i rispettivi effetti potrebbe essere fondamentale per sviluppare terapie contro la patologia da α-syn indotta da ictus.

ABSTRACT

Stroke remains to be one of the leading causes of death and disability worldwide, with limited therapeutic options. Vascular damage and inflammation correlate with stroke severity and worse outcomes in patients. Alpha-synuclein (α-syn), a neuronal protein widely known for its pathogenic role in chronic neurodegenerative diseases, such as PD, is also involved in acute brain damage following ischemic stroke by modulating vascular injury and recovery processes. Here, we investigated the impact of ischemia-induced α-syn pathology in brain damage and recovery in acute, sub-acute and chronic phases of injury *in vivo*. We also developed an *in vitro* non-cellular model of α-syn aggregation in ischemia mimicking conditions to test the effect of candidate therapeutic compounds/drugs.

Focal transient cerebral ischemia was induced in C57BL/6RCC wild-type and C57BL/6S null mice with spontaneous deletion of α-syn by unilateral transient occlusion of the middle cerebral artery (tMCAo) for 30 minutes. Mice were evaluated for sensorimotor deficits at day 9, anxiety like phenotype and overall locomotor function at day 28 using EPM, spatial learning and memory using Barnes maze at day 30-35 and overall survival as a measure of stroke outcomes. MRI was used to longitudinally analyse infarct size, blood flow and brain edema. We observed a better overall survival in null mice despite comparable sensorimotor deficits during the sub-acute phase of tMCAo. However, α-syn null mice showed reduced time spent in centre zone of EPM apparatus, suggesting a reduced explorative phenotype and impaired learning compared their sham controls in Barnes Maze test, suggesting a role for endogenous α-syn in brain recovery after ischemic stroke. Furthermore, α-syn null mice showed bigger lesions, cerebrovascular flow deficit and brain edema compared to wild type mice in MRI analysis at 3 days after tMCAo followed by a marked recovery in all the parameters at 7 days, suggesting the presence of a time dependent effect of α-syn toxicity in ischemic vasculature. To evaluate the distinct role of endogenous and toxic α-syn in brain vasculature, we reproduced our invitro model of ischemia-reperfusion injury in microvascular endothelial cells in the presence or absence of monomeric α-syn supplemented in the beginning of ischemia or during reperfusion. We observed α-syn treated ischemic cells showed increased *ICAM-1* induction compared to non-treated ischemic cells and treatment with monomeric α-syn reduced *ICAM-1* expression to untreated levels, suggesting a toxic effect for ischemia preconditioned α-syn and a beneficial effect of monomeric α-syn. To better characterize the effect ischemic condition in α-syn protein alterations and screen therapeutic compounds, we first performed an *in vitro* aggregation of α-syn in acidic pH (ischemic only condition) followed by co-aggregation of fibrils generated in acidic pH with monomeric α-syn in physiologic pH (reperfusion condition) in the absence of Clusterin and doxycycline. We observed a compact beta sheet structure, and higher seeding capacity of ischemic aggregates compared to those

generated in buffer with physiologic pH We also observed that the aggregation of α-syn was completely inhibited by Clusterin in ischemia-reperfusion mimicking condition and by doxycycline when aggregated in buffer with physiologic pH.

Overall, our data suggests that α-syn impact on brain injury or recovery after ischemic stroke can be influenced by a time dependent generation of its toxic species. We believe that α-syn might play a essential role in the acute response and delayed recovery after ischemic stroke. While, during sub-acute and chronic phases, the generation of its toxic species due to the ongoing ischemic injury may be detrimental and impair brain remodeling. The availability of experimental models that can dissect and recapitulate these dynamic changes in α-syn and respective effects might be essential to develop therapies against stroke-induced α-syn pathology.

TABLE OF CONTENTS

ITALIAN ABSTRACT 2

ABSTRACT 4

1. INTRODUCTION 11

1.1 ISCHEMIC STROKE 11

1.2 PATHOPHYSIOLOGY OF ISCHEMIC STROKE 12

1.3 BBB AND ITS DISRUPTION FOLLOWING CEREBRAL ISCHEMIA 12

1.3.1 Structure and physiological function of BBB 12

1.3.2. BBB's disruption in cerebral ischemia 13

1.3.3. Mitochondrial dysfunction and oxidative stress in ECs 13

1.3.4. Inflammation in BBB damage after stroke 15

1.4 VEGFS AND VEGF RECEPTORS 16

1.5 MATRIX METALLOPROTEASES (MMPS) 17

1.6 ANGIOGENESIS AND VASCULAR REMODELLING AFTER STROKE 18

1.7 ALPHA-SYNUCLEIN 19

1.7.1. Alpha-synuclein (α-syn) structure and function 19

1.7.2. Alpha-synuclein role in ischemic stroke 20

1.7.3. Alpha-synuclein in endothelial (ECs) and perivascular cells 22

1.7.5 Modeling a-syn aggregation in test tube 24

1.7.8 Targeting a-syn aggregation with inhibitors 25

1.7.10 Alpha-synuclein expression, oligomerization and association with cortical vessels following ischemic stroke 26

2. AIM OF THE STUDY 29

3. MATERIAL AND METHODS 31

3.1 Animals 31

3.2 tMCAo (transient ischemia) model 31

3.3 Inclusion/exclusion criteria 32

3.4 Health monitoring 33

3.5 Behavioral deficits 33

3.6 Elevated Plus Maze (EPM) 34

3.7 Barnes Test 34

3.8 Brain collection 35

3.9 Magnetic Resonance Imaging (MRI) acquisition 35

3.10 Diffusion-Weighted Imaging (DWI/IVIM) 36

3.11 T2-weighted imaging (T2WI) 36

3.12 The ITK-SNAP software 36

3.13 *In vitro* ischemia 37

3.14 Quantitative Real-time-PCR (qRT-PCR) 37
3.15 Aggregation assay 38
3.16 Statistical analysis 38
4. RESULTS 39
In vivo 39
4.1 Alpha-synuclein deficiency improved mice survival after 30-min of tMCAO 39
4.2 Alpha-synuclein null mice show increased infarct volume at 3 days but an enhanced recovery at 7 days after tMCAo 40
4.3 Alpha-synuclein null mice show worsened brain ischemia induced cerebrovascular flow deficit at 3 days after tMCAo, but enhanced recovery after 7 days 41
4.4 Alpha-synuclein null mice exhibited increased vasogenic edema at 3 days following tMCAO, but demonstrated accelerated edema resolution by day 7 43
4.5 The absence of ischemia induced α-syn toxicity did not attenuate long-term functional and cognitive deficits after tMCAo 45
In vitro 47
4.6 Extracellular ischemia altered α-syn further exacerbates I/R injury while monomeric α -syn reduced inflammation in microvascular endothelial cells 47
4.7 Hypoxia promotes the aggregation of monomeric α-syn in non-cellular condition 48
4.8 Alteration of pH of buffer solutions mimics *in vivo* ischemia induced α-syn pathology 48
4.9 Clusterin and Doxycycline exert complete inhibition of α-syn self-aggregation in acidic and physiologic pH respectively in non-cellular condition 49
4.10 Alpha-synuclein fibrils produced at acidic pH exhibit superior seeding of monomeric protein 50
5. Discussion 52

LIST OF ABBREVIATION

ADC*: Apparent Diffusion Coefficient*

α-SYN: *Alpha-synuclein*

BBB: *Blood brain barrier*

CD: *Circular dichroism*

CSF: *Cerebrospinal fluid*

DALY: *Disability-Adjusted Life Years*

DAMP: *Damage-associated molecular pattern*

DOXY: *Doxycycline*

DWI: *Diffusion Weighted Imaging*

eNOS: *Endothelial nitric oxide synthase*

EGF: *Epidermal Growth Factor*

EPI: *Echo Planar Imaging*

ECM: *Extracellular matrix*

ECs: *Endothelial cells*

EPCs: *Endothelial progenitor cells*

EPM: *Elevated plus maze*

EPO: *Erythropoietin*

ER: *Endoplasmic reticulum*

ET: *Endothelin*

EVs: *Extracellular vesicles*

FBS: *Fetal bovine serum*

HIF-1 α: *Hypoxia-inducible factor 1*

ICAM-1: *InterCellular adhesion molecule*

IC: *Internal carotid artery*

LVOs: *Large vessel occlusions*

MCA: *Middle Cerebral Artery*

MMPs: *Matrix metalloproteases*

MRI: *Magnetic Resonance Imaging*

NAC: *Non-amyloid component*

NF-κB: *Nuclear factor κ-light-chain-enhancer of activated B cells)*

NO: *Nitric oxide*

NOX: *Nicotinamide adenine dinucleotide phosphate (NADPH) oxidase*

NVU: *Neurovascular unit*

OGD: *Oxygen-glucose deprivation*

PD: *Parkinson's disease*

PWI: *Perfusion Weighted Imaging*

PECAM-1: *platelet endothelial cell adhesion molecule*

pffs: *pre-formed fibrils*

PIGF: *placental growth factor*

RNS: *Reactive nitrogen species*

ROS: *Reactive oxygen species*

SHR: *Spontaneously hypertensive rats*

SN: *Substantia nigra*

TIMPs: *Tissue inhibitors of MMPs*

TJs: *Tight junctions*

TLR: *Toll-like receptors*

ThT: *Thioflavin T*

tMCAo: *Transient occlusion of middle cerebral artery*

TNF-α: *Tumor necrosis factor α*

tPA: *Recombinant tissue Plasminogen Activator*

VE: *Vascular Endothelin*

VEGF: *Vascular endothelial growth factor*

vWF: *Von Willebrand factor*

WHO: *World Health Organization*

WPBs: *Weibel-Palade bodies*

WT: *Wild-Type*

ZO: *Zonula occludens*

1. INTRODUCTION

1.1 ISCHEMIC STROKE

Stroke is a condition with a significant impact on the population in terms of mortality, disability, and social and economic costs. It is the third leading cause of death (after ischemic heart disease and COVID-19) and the fourth leading cause of DALYs (after COVID-19, ischemic heart disease, and neonatal disorders)[1]. Globally, in 2021, there were 93.8 million (95% UI 89.00–99.3) stroke survivors, 11.9 million (10.7–13.2) new stroke events, 7.3 million (6.6–7.8) deaths from stroke, and 160.5 million (147.8–171.6) DALYs (Disability-Adjusted Life Years [2].

According to the World Health Organization (WHO), stroke is defined as rapidly developing clinical signs of focal or global disturbance of cerebral function lasting more than 24 h (unless interrupted by surgery or death) with no apparent cause other than of vascular origin [3]. Stroke occurs either when a blood vessel supplying a brain region is clogged with a thrombus or embolus, as in ischemic stroke, which accounts for the vast majority (87%) cases, or when a blood vessel bursts and bleeds, as in hemorrhagic stroke that comprises 13% of all cases. Large vessel occlusions (LVOs), defined as blockages of the proximal intracranial anterior and posterior circulation, account for approximately 40% of acute ischemic strokes. Around 80% of LVOs occur in the territory of the Middle Cerebral Artery (MCA) or the Internal Carotid artery (IC)[4]. Insufficient blood supply following stroke restricts the delivery of oxygen and essential nutrients, causing energy failure, followed by secondary processes such as BBB disruption, infiltration of immune cells, and activation of the glial cells that culminates in the death of neurons and non-neuronal cells[5]. Currently, the only approved pharmacological therapy for acute ischemic stroke uses a clot dissolving agent, recombinant tissue Plasminogen Activator (tPA), administered alone or combined with endovascular therapy[6,7]. Despite treatment with tPA and endovascular therapy improves early clinical recovery, only a third of ischemic stroke patients receive these therapies due to a limited time window of effectiveness. Moreover, only 20%-30% of patients achieve complete recanalization after thrombolysis with tPA, while most patients evolve toward permanent ischemia [8]. Further adding to this challenge, reoxygenation of a previously ischemic brain during reperfusion therapy can paradoxically exacerbate cellular injury and dysfunction [9]. Hence, stroke remains a therapeutic challenge, and further studies are warranted to identify new therapeutic targets that promote the repair and regeneration of brain tissue damaged by ischemia and reperfusion.

1.2 PATHOPHYSIOLOGY OF ISCHEMIC STROKE

Ischemic stroke a series of pathophysiological events that occur in a time and space-dependent manner, ultimately leading to brain injury [9]. In the core of the ischemic territory, a region with severely compromised cerebral blood flow, irreversible cell death occurs due to energy deficit resulting in ion imbalance, mitochondrial failure, and activation of intracellular enzymes leading to the digestion of cellular structures and necrosis [10,11]. At the same time, in the ischemic penumbra, reduced blood flow is provided by arterial collaterals, producing a functionally impaired but viable tissue surrounding the ischemia core, making it salvageable to rapid therapeutic interventions [12]. However, brain tissue in the ischemic penumbra suffers from slow apoptotic cell death, excitotoxicity, and inflammation due to progressive ischemia or reperfusion injury. In addition to neuronal cell death, ischemia alone or followed by reperfusion causes early and progressive endothelial cell dysfunction and loss leading to vascular damage with resultant BBB leakage, cerebral edema, and hemorrhage that contributes to worsened outcomes in patients with ischemic stroke [13] also signifying the need for vessel protective and restorative therapies. In this regard, post-ischemic brain tissue activates signalling pathways associated with angiogenesis and repair of BBB in a limited way, which in human patients was correlated with improved functional recovery [13,14].

1.3 BBB AND ITS DISRUPTION FOLLOWING CEREBRAL ISCHEMIA

1.3.1 Structure and physiological function of BBB

The microvasculature of the brain forms a specialized structure known as the BBB, which is composed of highly specialized endothelial cells (ECs) basement membranes, pericytes, perivascular cells, and astrocytic endfeet (Figure 1) able to maintain homeostasis and shield the brain from blood-borne toxins or pathogens [15–18]. Since an elaborate tight junction (TJ) network between endothelial cells limits the paracellular flux of water-soluble molecules, the absence of fenestrae and low pinocytotic activity tightly regulates the transcellular transport of molecules across the BBB[15,16]. The TJ between ECs consists of transmembrane (claudins, occludin, and junctional adhesion molecules) and cytoplasmic proteins (zonula occludens (ZO) 1 and ZO-2, cingulin, AF-6, and 7H6) that link the transmembrane proteins to an actin cytoskeleton. Claudin 3 and 5 are the main components of the brain TJ network and are responsible for its restrictive property. Brain ECs are also interconnected through adherence junctions that are primarily composed of Vascular Endothelin (VE) -cadherin and platelet endothelial cell adhesion molecule (PECAM-1 or CD31).

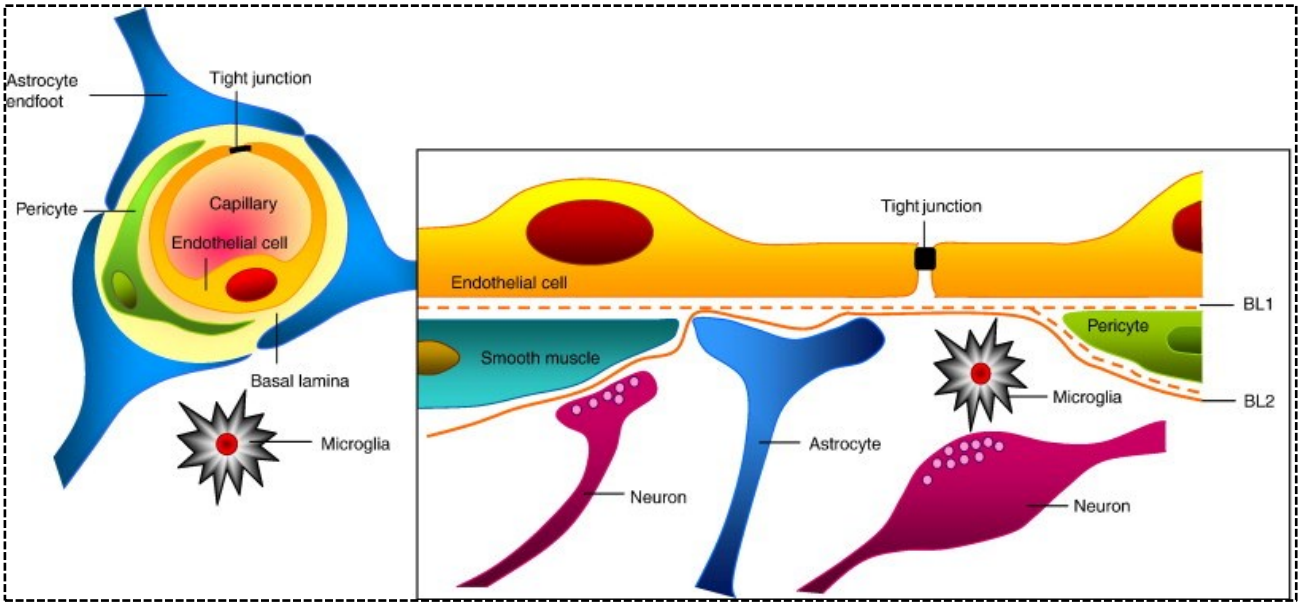


Figure 1. Schematic representation of the components of the BBB (From Abbott et al.,2010).

1.3.2. BBB's disruption in cerebral ischemia

Previous studies have shown that acute ischemic stroke causes a breakdown in the BBB that leads to the influx of blood components into the brain parenchyma resulting in edema and hemorrhagic transformation, which are detrimental to functional recovery in patients. In human patients, BBB disruption occurs within 2 days after stroke onset [19], while in experimental models of ischemic stroke, the breakdown was detected after 6 h of reperfusion [20]. In this context, Magnetic Resonance imaging has emerged as a valuable tool, offering the ability to visualize, characterize, and quantify biological processes through specific indices such as perfusion index (ADC, *apparent diffusion coefficient*) and S0 (vasogenic edema index). Several factors contribute to BBB breakdown after ischemia, including mitochondrial changes due to energy failure in ECs, apoptosis of ECs, systemic and local inflammation leading to elevated production of matrix metalloproteases (MMPs), and oxidative stress [20]. In addition, vascular permeability allows the infiltration of immune cells, such as neutrophils, into the brain from the plasma, amplifying neuroinflammation and neuronal injury[21,22].

1.3.3. Mitochondrial dysfunction and oxidative stress in ECs

The brain tissue depends on glucose as a primary energy source and hence requires a constant supply of blood flow to meet its energy demands. Cerebral ECs, which play a significant role in the proper function of the BBB, possess higher numbers of mitochondria than ECs in the periphery, making them vulnerable to mitochondrial dysfunction [23]. Additionally, brain ECs mitochondria are known to primarily be involved in cell signalling function by regulating and responding to various stimuli such as ischemia, thereby exerting a role in the modulation and maintenance of the BBB integrity [24]. Ischemia-reperfusion injury causes the formation of reactive oxygen species, ROS (e.g., superoxide

and hydrogen peroxide) and reactive nitrogen species RNS (e.g., nitric oxide and peroxynitrite) and the release of cytochrome c from mitochondria thereby leading to caspase 3 mediated degradation of ECs TJ proteins in vitro [25]. LPS and drug-induced mitochondrial dysfunction also compromised BBB integrity and worsened stroke outcomes in vivo [24]. Excessive accumulation of ROS/RNS damages lipids, proteins, DNA, and cytoskeleton causing cell death and tissue destruction. In particular, the brain is susceptible to ROS/RNS-mediated injury due to high amounts of lipids, low concentrations of antioxidants, high oxygen consumption, and higher iron levels [26,27]. Vascular oxidative stress has been documented in patients and animal models of hypertension, a major risk factor for stroke [28,29]. In the vasculature, ROS are known to disrupt vascular tone, promote platelet aggregation, induce ECs morphogenesis, and enhance production of matrix metalloproteases (MMPs) involved in the degradation of TJ proteins and BM components (Figure 2) thereby leading to BBB disruption [26]. Moreover, ROS are shown to activate transcriptional factors such as NF-κB (nuclear factor κ-light-chain-enhancer of activated B cells), thus leading to an increase in the expression of cell adhesion molecules such as *ICAM-1* and VCAM in ECs [30,31], further accelerating vascular inflammation and injury. Studies also indicated that ROS induces lysosomal dysfunction and activates autophagy in astrocytes and pericytes, contributing to BBB disruption (Figure 2). Furthermore, ROS are indicated to contribute to the accumulation of toxic forms of α-syn, which are implicated in neuronal degeneration [32].

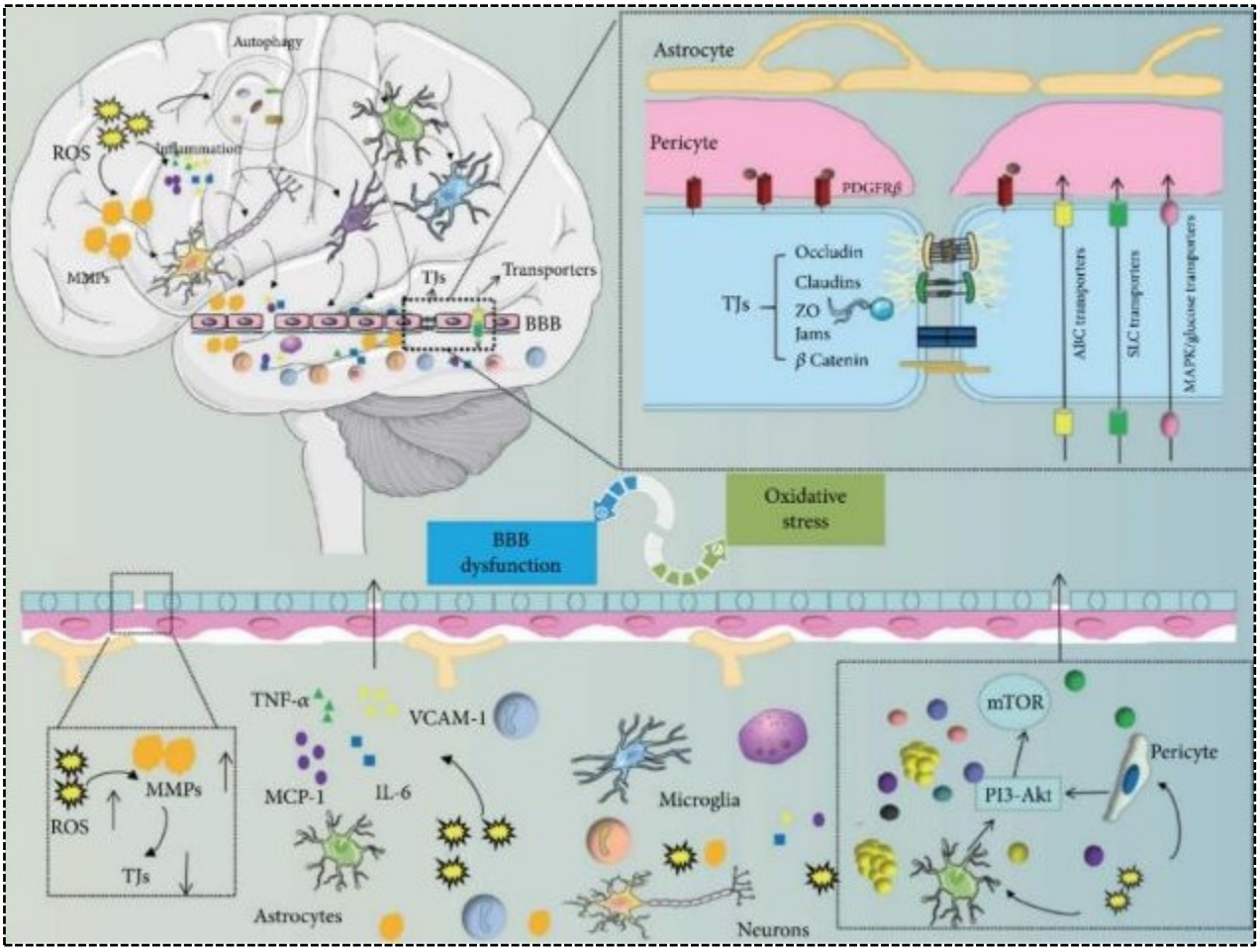


Figure 2. Schematic representation of main pathological pathways involved in ROS mediated BBB damage (from Song et.al., 2020).

1.3.4. Inflammation in BBB damage after stroke

Microglia, brain resident immune cells, are activated and proliferate during various phases of ischemic injury in the brains of patients and animal models of stroke [33]. The initial breakdown in the BBB following stroke is followed by the influx of peripheral immune cells into the cerebral parenchyma and the activation of glial cells such as microglia. This sets a cycle of enhanced pro-inflammatory response and further BBB damage [10,31]. ROS production by injured and activated cells during acute injury can produce cytokines and chemokines, further amplifying the inflammatory cascade, culminating in vascular damage and cell death [31]. The ischemic environment induces the acquisition of different phenotypes and functional states in microglia cells, allowing them to play distinct roles in the progression or resolution of brain damage that follows stroke [33]. Among the various phenotypes of microglia that are identified to date, classically activated microglia (M1) produce pro-inflammatory factors such as tumor necrosis factor α (TNF-α) interleukin (IL)-1β, interferon-γ (IFN-γ), IL-6, inducible nitric oxide -synthase (iNOS), and MMPs while alternatively activated microglia (M2) produce mediators that are anti-inflammatory and proangiogenic factors

including IL-10, transforming growth factor β (TGF-β), insulin-like growth factor, and vascular endothelial growth factor (VEGF) [34]. Moreover, following brief ischemia in rodents, microglia reduced their activity with retraction of their processes that were recovered upon reperfusion whereas, in permanent ischemia without reperfusion, extensive microglia loss was accompanied by enhanced infiltration of peripheral macrophages [35,36]. Moreover, activated glial and immune cells induce the expression of molecules such as vascular endothelial growth factors (VEGFs) and their receptors, MMPs, and endothelin (ET) in the ischemic penumbra.

1.4 VEGFS AND VEGF RECEPTORS

The VEGF family proteins comprise five members VEGF-A, B, C, D, and placental growth factor (PIGF) in mammals (Figure 3), which mediates their function through tyrosine kinase VEGF receptors and Neuropilin co-receptors (NRP-1 and 2) [37,38]. VEGF-A and VEGF-B and their receptors (VEGFR-1 and VEGFR-2) are expressed and secreted by neuronal and non-neuronal cells starting at 2h. They remained elevated over days to weeks following ischemia [39,40]. Hypoxia-inducible factor 1 (HIF-1α), a master transcription factor involved in the adaptation of cells to low-oxygen levels, induces the expression of VEGF-A after stroke by a direct effect on VEGF gene or indirectly through erythropoietin (EPO) [39–41]. Inflammatory cytokines and lactate are also described to regulate VEGF-A in stroke. VEGF-A is the most prominent isoform and by signalling via VEGFR-1 (Flt1), it regulates ECs proliferation, migration, survival, and neuroprotection while by signalling via VEGFR2 (KDR/Flk-1), it mediates vascular permeability and angiogenesis following hypoxic-injury. VEGF-A induces the expression of soluble forms of VEGFR-1, which binds and sequesters soluble VEGF molecules, subsequently inhibiting angiogenic signalling [42]. In contrast, VEGF-B is known to only bind to VEGFR-1, exhibiting a neuroprotective role [43]. The role of VEGF in stroke is still controversial. VEGF has shown to have a direct role in neuroprotection when administered to neurons in an in vitro ischemia model or when administered as s topical agent on the surface of cortical vessels [39]. However, excessive VEGF levels have shown to induce vascular permeability by promoting the formation of fenestrations and caveolae in ECs and disrupting inter-endothelial junctions following hypoxia and inhibiting VEGF signalling during the early phase of stroke. It has been found to reduce BBB breakdown, brain edema, and infarct size in a rodent model of MCA occlusion [44,45].

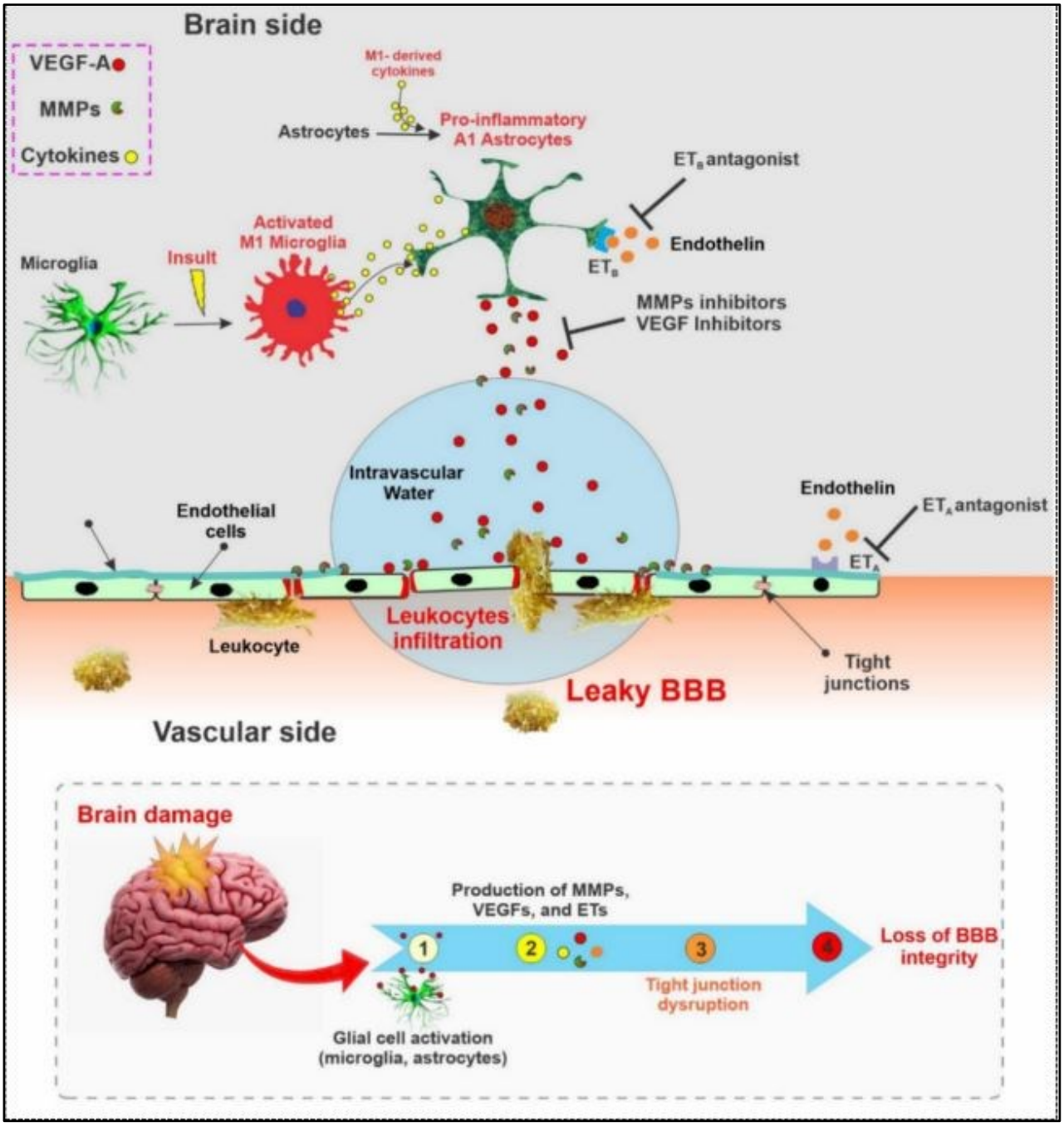


Figure 3. Schematic illustration of events that leads to BBB disruption following injury (from Wang et.al., 2007).

1.5 MATRIX METALLOPROTEASES (MMPS)

Metalloproteases are zinc-dependent matrix-degrading enzymes expressed by neuronal and non-neuronal cells and are involved in tissue remodelling under physiological and pathological conditions [46]. In the CNS, the expression of MMPs is tightly controlled by transcriptional regulation, posttranslational modification, and interaction with tissue inhibitors of MMPs (TIMPs). Most MMPs are transcribed at significantly lower levels under basal conditions and are induced upon stimulation by cytokines, chemokines, and growth factors. Upon cell activation, MMPs are translated as inactive

enzyme precursors/zymogens and are activated by proteolytic and non-proteolytic factors such as ROS [46]. Excessive induction and activation of MMP 2 and 9 are associated with BBB leakage, inflammation, and neuronal death after stroke onset [20]. However, recent studies have shown that MMPs play a beneficial role in sub-acute phases of stroke by promoting the release of trophic factors such as VEGF from the extracellular matrix, promoting angiogenesis, and neurovascular remodelling [47].

1.6 ANGIOGENESIS AND VASCULAR REMODELLING AFTER STROKE

Recovery after ischemic stroke, even after a complete recanalization therapy, is limited; hence most patients will suffer from a permanent neurological deficit. Endogenous neurogenesis [48] and angiogenesis [49] have been activated and are suggested to contribute to brain repair and spontaneous functional recovery after stroke. Post-stroke angiogenesis is the formation of new vessels by sprouting from pre-existing vessels, which will restore blood flow in the ischemic region, support newly generated neurons and nerve connections, and clean up damaged tissue in the ischemic core [50]. Additional mechanisms, such as vasculo-genesis mediated by circulating endothelial progenitor cells (EPCs) have also been described to contribute to new vessel formation following ischemia [51,52]. In humans, angiogenesis occurs 3-4 days after stroke, while most vascular genes are upregulated within an hour after reperfusion and remain elevated for several days [49–53]. Recent studies using transient focal ischemia in rodents have demonstrated that angiogenesis and axonal growth are activated only at the border of the ischemia core but not penumbra after 7 days and 28 days post-reperfusion, respectively [54]. Several factors, including VEGF and its receptor VEGFR-2, Angiopoietin-1 and its receptor Tie2, and eNOS (endothelial nitric oxide -synthase), are described to regulate post-stroke angiogenesis and non-pharmacological interventions such as exercise have been shown to play a beneficial role in stroke recovery by improving the levels of these trophic factors. Higher density of micro-vessels is correlated with longer survival, and it improves functional recovery in human stroke patients and rodents with focal ischemia, respectively [49,55]. However, controversy remains regarding the precise role of angiogenesis in cerebral ischemia.

1.7 ALPHA-SYNUCLEIN

1.7.1. Alpha-synuclein (α-syn) structure and function

Alpha-synuclein (α-syn) is a small (14kDa), naturally unfolded protein abundantly expressed in the brain primarily by neurons [56,57] and, to a lesser extent, by glial and endothelial cells (ECs) [58–60]. The physiological function of α-syn remains equivocal, yet the protein is described to play a role in - synaptic vesicle trafficking, neurotransmitter release, mitochondrial homeostasis, autophagosome/lysosomal function, and cytoskeletal reorganization in neurons [57,61–64]. The full-length α-syn isoform comprises 140 amino acids, and its sequence is divided into three regions (Figure 4). The amphipathic amino-terminal domain is a highly conserved region, important for membrane binding, and consists of sites of familial Parkinson's disease mutations such as A30P, A53T, and E46K [62,64]. The intermediate-hydrophobic region, also known as the non-amyloid component (NAC), promotes the aggregation of the protein and it is necessary and sufficient for α-syn fibrillation [65]. Finally, a negatively charged carboxyl-terminal domain contains residues for the most common post-translational modification of the protein, including serine-129 sites. It interacts with the N-terminal domain to form an aggregation-resistant structure [66]. α-syn is described as a natively disordered protein that exists in monomeric form[67] or a stable tetramer [68] when purified at neutral pH. Rapid environmental changes can induce the formation of partially folded intermediates or kinetically trapped transition states that are prone to aggregation [69]. With aging, the α-syn levels increase and undergo enhanced pathogenic modifications, including oxidative damage, which can promote the formation of high molecular soluble or insoluble aggregates, such as oligomers, protofibrils, or fibrils [64,70]. Sub-cellular localization of α-syn has shown that the protein is found in pre-synaptic terminals and cellular organelles such as the nucleus [71–73]. Notably, levels of nuclear α-syn and its binding to chromatin increase following oxidative stress, suggesting its role in the transcriptional regulation of various genes, particularly under pathological conditions [71,73–75]. α-syn has also been shown to localize at mitochondrial membranes and to mediate cytochrome C's release and nitric oxide (NO) production, leading to oxidative stress and apoptosis, the main hallmarks of neurodegenerative diseases [76].

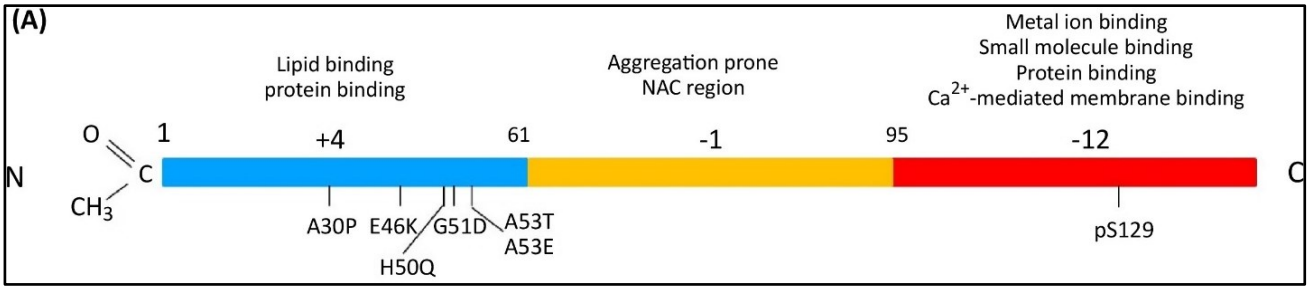


Figure 4. Schematic representation of the full-length 140 amino acid α-syn protein (From D. Stephens et.al., 2019).

Moreover, α-syn null mice displayed a reduced number of dopaminergic neurons in the substantia nigra, suggesting the role of endogenous α-syn in preventing death and promoting the differentiation of neurons during development [77]. α-syn is well known for its pathogenic role in chronic neurodegenerative diseases such as Parkinson's disease (PD) and, recently, acute brain injury such as stroke. α-syn is a major component of Lewy bodies and Lewy neurites which are pathological hallmarks of PD [78]. In PD, α-syn deposition is thought to play a pathogenic role in inducing progressive neuronal degeneration in the brain and periphery underlying the onset of motor and non-motor deficits, respectively [79,80]. Interestingly, both monomeric and aggregated α-syn can be transferred from cell-to-cell, (neuron-neuron, neuron-glia) and can be detected in body fluids of mice and PD patients such as cerebrospinal fluid (CSF), blood plasma, and in neuronal cell culture media [81–83]. In addition, the release of α-syn is enhanced after cellular stress [84]. Exocytosis, endocytosis, extracellular vesicle (EVs), carrier-mediated transports, and tunneling nanotubes are described as the primary mechanisms for transmitting the protein between cells [85–87]. To this end, blockage in brain fluid clearance mechanisms such as glymphatic and lymphatic drainage pathways, results in α-syn accumulation in the brain parenchyma and contributes to the progression of PD-like phenotype in transgenic mouse models [88]. α-syn has also shown to increase after stroke and to mediate post-stroke brain damage, suggesting its role in acute injury [89–92].

1.7.2. Alpha-synuclein role in ischemic stroke

Cerebral ischemia may provide a suitable condition for α-syn induction and aggregation by inducing vascular damage, mitochondrial dysfunction, endoplasmic reticulum (ER) stress, and oxidative stress. Various studies have demonstrated the role of α-syn after ischemic injury (Figure 5). In this regard, brief (30 min) proximal unilateral middle cerebral artery occlusion followed by 24 h reperfusion in young wild-type (wt) mice induced oligomerization and aggregation of α-syn; 30 min occlusion followed by 72 h reperfusion in the distal MCA produced enhanced selective neuronal loss in transgenic mice that overexpressed mutant (A30P) α-syn compared to non-transgenic mice, suggesting an increased susceptibility to ischemia in these mice [90]. Moreover, in vitro oxygen-glucose

deprivation followed by reoxygenation in rat pheochromocytoma (PC12) cells upregulated α-syn levels, increased its nuclear localization, and mediated cell death [89]. Similarly, unilateral 60 min occlusion of MCA followed by 1 day or 7 days of reperfusion in spontaneously hypertensive rats (SHR) induced α-syn levels with increased nuclear translocation, and this was in line with enhanced immunoreactivity for α-syn in human brain sections, which were diagnosed to have an ischemic stroke without comorbidities [89]. On the other hand, 1 day of unilateral MCA occlusion without reperfusion in wt rats led to neuronal cell death and reduced α-syn protein levels in the ischemic cerebral cortex [93]. Additionally, the knockdown of the α-syn gene using siRNA in SHR or mice knock-out for α-syn gene reduced infarct volume, rescued mitochondrial dysfunction, and improved motor function during the sub-acute phase and overall survival [89]. Deregulation in the transcriptional control of α-syn has been shown to underly its induction in SHR after stroke and, more specifically, the downregulation of miR-7a-5p (miR-7), a micro-RNA which is known to repress the expression of α-syn was detected following stroke [94,95]. To this end, treatment with miR-7 mimic oligonucleotides ameliorated brain damage associated with induced α-syn after tMCAo in SHR, similar to α-syn loss [94]. Higher levels of oligomeric and phosphorylated α-syn were detected in red blood cells (RBCs) of patients with acute ischemic stroke, suggesting an induction and release of the protein possibly from ischemic neurons, however their role in ischemia is not yet known [91]. Previous studies have shown that erythrocyte-derived exosomes containing α-syn from PD cases induced microglial activation and contributed to brain inflammation [96]. In addition, a pioneering study demonstrated that hippocampal ischemia in gerbils increased α-syn immunoreactivity around hippocampal blood vessels during early periods suggesting a potential role of the protein in vascular pathology during a stroke [97].

Model	Duration	Species	Levels	Observations	Ref.
Global ischemia	5 min	Gerbil	upregulated	↑ a-syn around blood vessels in CA1 on day 4; ↑ a-syn $^{+}$ tubal structures on month 6	(98)
HI	90 min	Rat	upregulated	2-fold increase 2 h after HI	(99)
Global ischemia	5 min	Gerbil	upregulated	↑ a-syn in CA1 in aged gerbil; SOD1 inhibited α-Syn	(100)
Global ischemia	30 sec	Mouse	N/A	a-syn $^{-/-}$ increased brain PG formation following ischemia	(101)
tMCAo	30 min	Mouse	upregulated	Brief ischemia induced a-syn aggregation, worsened damage	(93)
tMCAo	60–90 min	Rat, Mouse	upregulated	↓ a-syn reduced infarcts and improved neurological recovery	(89)
pMCAo	1 day	Rats	Downregulated	Neuronal loss associated with reduced levels	(94)

Figure 5. Summary of studies conducted to understand the role of α-syn in ischemia (modified from Kim T and Vemuganti R, 2017)

1.7.3. Alpha-synuclein in endothelial (ECs) and perivascular cells

Endothelial cells constitute the innermost lining of the vascular system [98,99]. Cerebral ECs play a role in the formation of the BBB, the regulation of immune cell trafficking, vascular hemostasis, and support cell survival and proliferation during development and following transplantation. In the brain, ECs maintain the BBB through interactions with neurons, pericytes, astrocytes, and macrophages in the neurovascular unit (NVU) and by secreting endothelial basement membrane that provides additional physical barrier [15–17,100,101]. BBB disruption and endothelial cell dysfunction have been identified in stroke and PD, where changes in α-syn have also been described [102]. α-syn is known to be expressed in cerebral ECs in a gradient-dependent manner where leptomeningeal ECs contain higher levels of the protein, while intra-parenchymal and capillary ECs show lower and no expression, respectively [59,102]. Moreover, EC lines, including those derived from cerebral micro vessels, express and release α-syn [59,103–105]. Subcellular localization of α-syn in ECs using transmitted-electron microscopy identified the protein near Weibel-Palade bodies (WPBs), intracellular granules that store chemokines, cytokines, and adhesive molecules and release them up on stimulation by agonists such as VEGF in order to modulate ECs response to injury [104–106]. The role of α-syn in ECs

function has yet to be fully understood. In vitro studies on ECs using wt and mutant α-syn demonstrated the role of the protein as a negative regulator of the release of factors implicated in immune cell infiltration, such as von Willebrand factor (vWF) and P-selectin from WPBs [104–107]. A recent study showed endogenous and recombinant monomeric α-syn plays a role in maintaining vascular integrity under basal conditions by promoting the production of endothelial NO (eNOs) and suppressing the production of VCAM 1 [105]. Moreover, aging-associated vascular dysfunction was attributed to the loss of function of α-syn in ECs [105]. In PD, deposition of toxic forms of α-syn is associated with chronic brain inflammation with high levels of pro-inflammatory cytokines such as TNF-α and IL-1β [108] that are known to activate the NF-kB and activator protein 1 (AP-1) pathways which are involved in the expression of VCAM 1 and *ICAM-1*[109] (Figure 6).

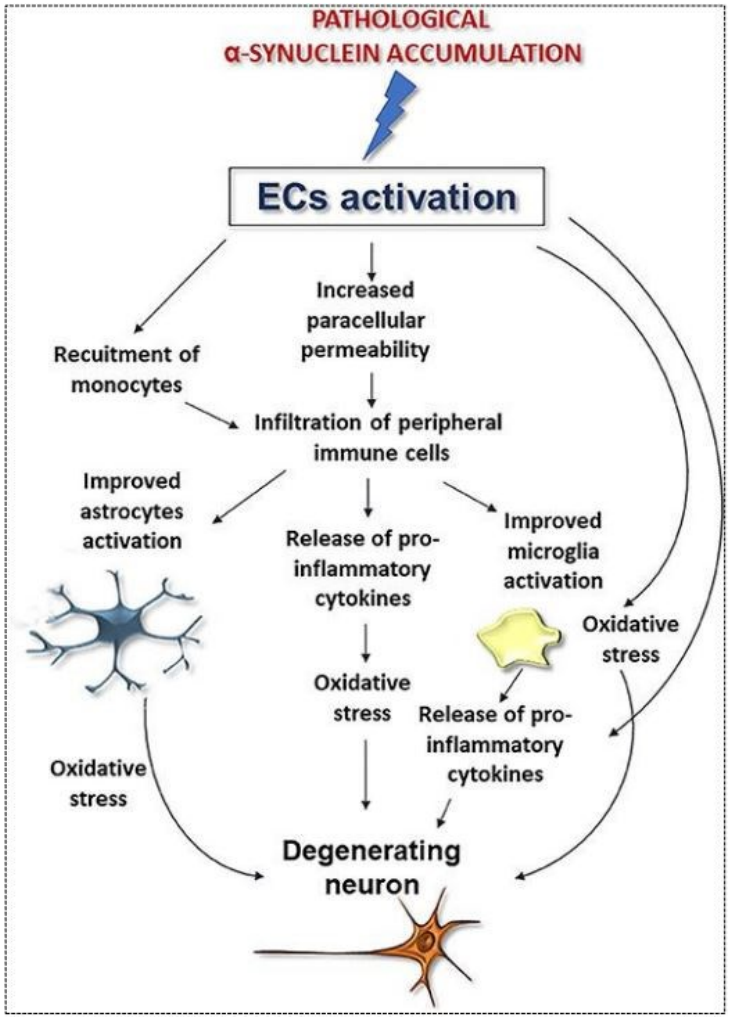


Figure 6. Schematic representation of possible hypothetical mechanisms of how α-syn induced ECs activation may lead to inflammation and neuronal degeneration (from Bogale et.al., 2021).

Furthermore, α-syn pre-formed fibrils (pffs) have shown to downregulate the expression of TJ proteins such as occludin and of zonula occludens 1 (ZO-1) without triggering endothelial dysfunction or release of pro-inflammatory cytokines from ECs[103]. In line with this, recent evidence

from a study using a human brain-chip model of the substantia nigra (SN) showed that α-syn fibrils could induce increased paracellular permeability, upregulate the expression of genes involved in inflammation, oxidative stress, autophagy, efflux system, extracellular matrix deposition and downregulate genes that encode for TJ proteins in ECs [110]. Furthermore, the brains of PD patients show signs of endothelial degeneration, loss of TJ proteins, and reactive angiogenesis in the nigrostriatal system where α-syn deposition is evident [103,111–113]. Moreover, studies have shown that perivascular cells such as pericytes play a major role in α-syn-associated vascular dysfunction [114–117].

1.7.5 Modeling a-syn aggregation in test tube

The misfolding of α-syn into amyloid fibrils is a hallmark of neurodegenerative diseases. Amyloid fibril formation is a critical event in the pathogenesis of α-synucleinopathies, such as Parkinson's disease and dementia with Lewy bodies. This process exhibits sigmoidal kinetics, characterized by a lag phase, exponential growth, and a plateau. The addition of pre-formed fibrils ("seeds") to the reaction mixture significantly accelerates fibril formation, highlighting the role of nucleation-dependent polymerization [118]. The introduction of seeds to the system substantially reduces the lag phase, demonstrating the catalytic effect of seeds on accelerating nucleation. Throughout this phase, unstructured α-syn monomers engage in dynamic interactions, forming a heterogeneous pool of loosely associated oligomers. This transformation is characterized by the rearrangement of parallel β-sheet structures, stabilized by intermolecular hydrogen bonds. Once nucleation occurs, fibril elongation proceeds through the addition of monomeric α-syn to the fibril ends. Upon reaching a critical length, fibrils can undergo fragmentation due to mechanical stress or intrinsic instability. This fragmentation generates new fibril ends, which act as additional nucleation sites in a process known as secondary nucleation. This mechanism significantly enhances fibril propagation and contributes to the exponential growth phase observed in the sigmoidal curve. The formation of β-sheet-rich structures is stabilized by hydrogen bonds and hydrophobic interactions. Oligomers that successfully adopt this amyloid conformation act as nuclei for fibril elongation [118]. Alpha-synuclein fibrils are highly hydrophobic structures characterized by a high β-sheet content. Their formation can be monitored by assessing changes in protein conformation or oligomerization state. Since the study of these processes in vivo or within cellular environments presents significant challenges, quantifying fibrillization in solution is more feasible. This is commonly achieved using fluorescent probes that respond to environmental rigidity or spectroscopic techniques that report on protein conformation, such as circular dichroism (CD) spectroscopy. Among the most widely used methods for detecting α-syn aggregates, the application of the small fluorophore Thioflavin T (ThT) is a reliable tool. This dye consists of donor and acceptor aromatic rings linked by a single bond, allowing free rotation and resulting in minimal fluorescence in aqueous environments. However, upon intercalation into the

structurally rigid β-sheet-rich environment of amyloid fibrils, ThT fluorescence undergoes a significant increase, making it a valuable tool for monitoring fibril formation [118].

1.7.8 Targeting a-syn aggregation with inhibitors

The role of Clusterin in the α-syn aggregation process has been the focus of recent investigations. Clusterin is a chaperone protein widely distributed throughout the body and plays a key role in binding unfolded proteins, thus helping to maintain them in a soluble state. Its function is similar to other small heat shock proteins (Hsp), such as Hsp27 and αβ-crystallin, which are known for their protective roles in cellular stress [119]. Clusterin is recognized as a crucial neuroprotective factor in the brain, particularly in the context of brain injury and stroke. However the levels of expression of the protein were found comparable to controls when analysed after ischemic stroke[120]. In both *in vitro* and *in vivo* studies, Clusterin has been shown to bind amyloid-β (Aβ) peptides, preventing their aggregation and facilitating their clearance through lipoprotein receptor-mediated internalization and subsequent lysosomal degradation. To investigate the functional involvement of Clusterin in the α-syn aggregation process, *small interfering RNA* (siRNA) has been utilized to down-regulate Clusterin expression. Under these conditions, an increase in high-molecular-weight (HMW) α-syn species was observed, both when α-syn was overexpressed alone and when proteome instability was induced. These findings suggest that Clusterin plays a dynamic role in modulating the aggregation of α-syn [121]. Moreover, whether Clusterin influence α-syn aggregation, in ischemic condition and reperfusion injury still unknown. Doxycycline is a broad-spectrum antibiotic belonging to the tetracycline class, which has been reported to exhibit neuroprotective properties [122]. These effects are believed to be related to its anti-inflammatory actions, like those of minocycline, another tetracycline antibiotic. In animal models of Parkinson's disease, tetracycline derivatives have demonstrated the ability to protect dopaminergic neurons in the substantia nigra, potentially by modulating the glial response in the 6-OHDA animal model of PD [123,124]. Moreover, doxycycline has been shown to inhibit the fibril formation of amyloid beta (Aβ), prion protein (PrP), β-microglobulin, and α-syn, suggesting its potential to mitigate protein aggregation in neurodegenerative diseases. The neuroprotective effects of doxycycline have been well-documented in various model systems, but the exact mechanisms of its action remain unclear. Recent findings have demonstrated that doxycycline reduces the formation of α-syn inclusions by inhibiting the seeding process and disrupting existing seeds, as confirmed by Thioflavin T (ThT) seeding assays. Additionally, doxycycline has been shown to inhibit mitochondrial reactive oxygen species production. Importantly, in vivo studies have demonstrated that doxycycline alters the cellular distribution of α-syn inclusions in dopaminergic neurons and restores motor function in models of neurodegeneration [125]. Previous studies showed that Doxycycline is also involved in vascular remodelling after ischemic stroke[126], reducing brain damage

and improving blood flow in the ischemic hemisphere. This could be due to the interaction between the molecule with toxic aggregates of α-syn produced after the ischemic event, promoting it as a possible pharmacological target.

1.7.10 Alpha-synuclein expression, oligomerization and association with cortical vessels following ischemic stroke

The present thesis grounds on previous observations of ours that aggregated α-syn: 1) is induced in a mouse model of ischemic stroke and 2) targets the ischemic blood vessels contributing to lesion expansion. Namely, in our previous study (Bogale et al, under revision, figure 7), we assessed α-syn mRNA expression following tMCAo and 48h of reperfusion. It showed significant increase in α-syn mRNA expression in the cortex ipsilateral to tMCAo vs the contralateral area (*2.148 ± 0.219, mean fold-change to contra-lateral cortex* ± SD, figure 7a). Interestingly, western blot analysis comparing the levels of total and oligomeric α-syn in cortex ipsilateral and contralateral to tMCAo, showed that although the total levels of α-syn were not different between non-ischemic and ischemic cortices, the latter exhibited a significant accumulation of oligomeric α-syn species (100kDa, red box). The optical density ± SD of 100kDa band was *0.887 ± 0.326* in ipsilateral cortices vs *0.326 ± 0.095* in the contralateral ones in C57BL/6Jmice at 48h after stroke. Interestingly, the elevation of oligomeric α-syn was sustained even at 7 days after tMCAo (*0.965 ± 0.169 vs. 0.305 ± 0.241*, figure 7b and 7c). To understand the cellular localization of α-syn after tMCAo, Alpha-synuclein, PSD-95 (a post-synaptic marker), CD31 (vessel marker) were immunolabeling plus DAPI-based nuclear staining on brain sections, which were then analyzed by confocal microscopy (figure 7d). In contralateral cortices, α-syn was localized at pre-synaptic terminals, as supported by the localization in proximity to the post-synaptic marker PSD-95 (figure 7d). Interestingly, in the tMCAo side (figure 7d, 3D renderings) α-syn was found to progressively accumulate inside perivascular cells at 48h and on blood vessels at 7d (figure 7d). At this point, PSD-95 positive puncta appeared to decrease in the ipsilateral side, compatible with the occurrence of synaptic degeneration and loss.

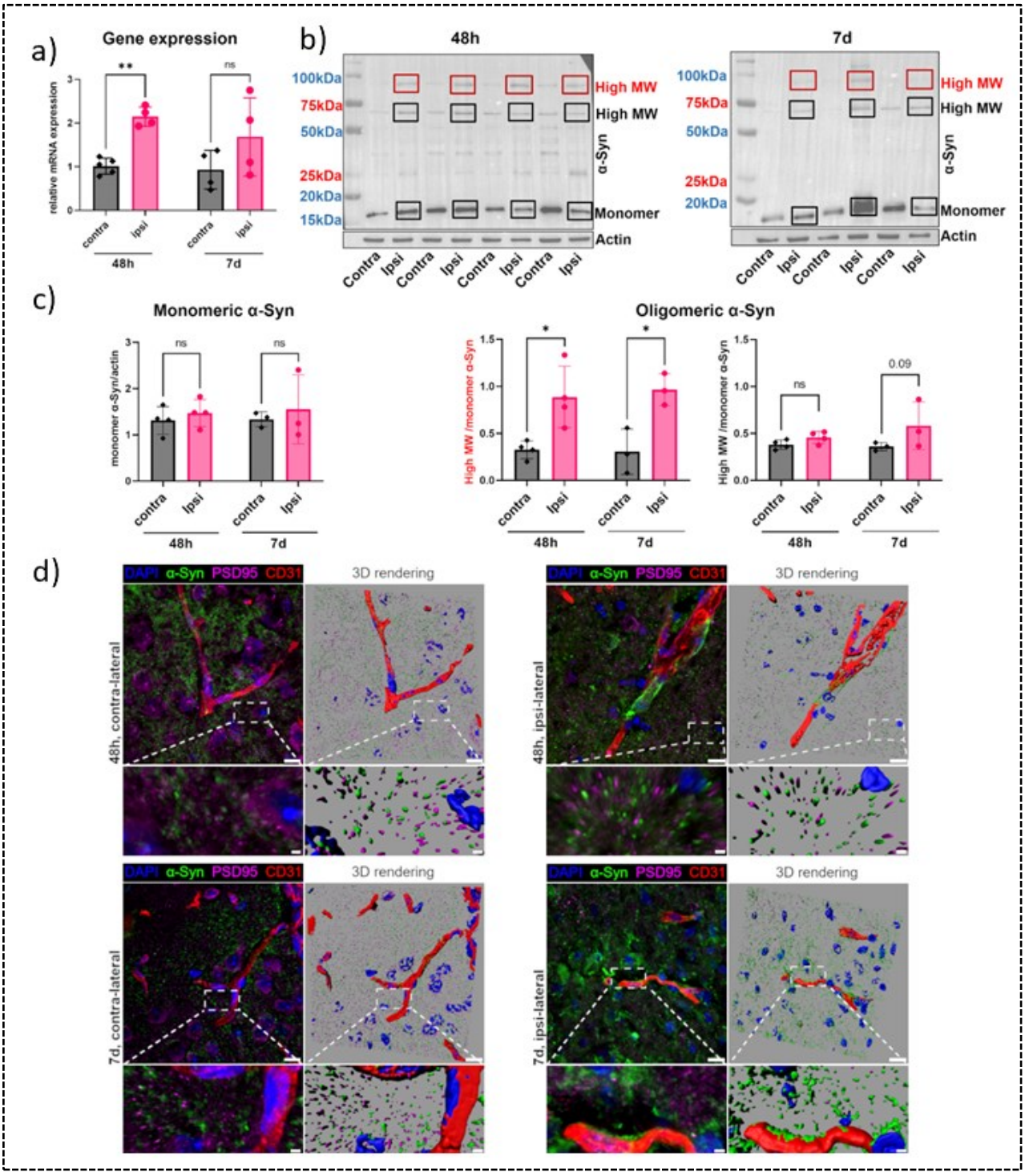


Figure 7. Alpha-synuclein mRNA increase, oligomerization and deposition on cortical vessels following stroke. a) Relative expression of *SNCA* in ipsilateral cortex of tMCAo mouse 48h and 7 days after cerebral ischemia compared to contralateral cortex (n=4). b) Western blotting for α-syn and β-actin from contralateral and ipsilateral cortex of WT mice (n=4). c) Densitometric quantification of western blot images in C for α-syn monomeric and oligomeric protein levels 48h and 7 days after ischemic stroke. d) Immunofluorescence microphotographs of ischemic and contralateral cortex of C57BL/6J mice labeled for α-syn (green), PSD95 (purple), CD31 (red) and

nuclei (blue) at 48h and 7 days after tMCAo. Scale bars 10 μm in the upper panels, 2 μm in the bottom magnified panels. Data are presented as individual values ± SD and analyzed by two-way ANOVA multiple comparisons followed by Sidak's post hoc test, *$p < 0.05$, **$p < 0.01$, ns= not significant (Bogale et al., under revision).

2. AIM OF THE STUDY

This project was conducted at the "Istituto di Ricerche Farmacologiche Mario Negri" in Milan and was focused on the study of the ischemic stroke, a pathology with a significant public health and socio-economic burden globally.

Current therapeutic options, including thrombolytic agents and mechanical thrombectomy, are constrained by a narrow therapeutic window, reperfusion injury and limited effect in tissue reperfusion and patient recovery despite successful removal of ischemic stroke clots. Therefore, identifying novel therapeutic targets is crucial to limit reperfusion injury and to improve post-recanalization outcomes after ischemic stroke.

Alpha-synuclein (α-syn), a small, widely expressed protein, is induced and aggregates after ischemic stroke, contributing to brain damage by promoting vascular damage or impairing vascular recovery. However, little data exist on the distinct role of physiological or toxic α-syn in long-term recovery after ischemic stroke. Moreover, approaches to reduce α-syn expression are challenging to use clinically and risk compromising the beneficial physiological function of the protein. Hence, there is a need for novel approaches to reduce α-syn aggregation and resulting acute and long-term brain injury after ischemic stroke.

The aim of this study was to investigate the role of α-synuclein (α-syn) in acute and long-term recovery after ischemic stroke *in vivo*. C57BL/6RCC (WT) and C57BL/6S (α-syn null) mice were subjected to transient middle cerebral artery occlusion (tMCAo) for 30 minutes and evaluated for survival, sensorimotor deficit using neuroscore, anxiety-like phenotype and overall locomotor function using elevated plus maze (EPM) and spatial learning and memory using Barnes maze. Magnetic resonance imaging (MRI) was used to analyse differences in lesion volume, blood flow (apparent diffusion coefficient, ADC) and S0 (vasogenic edema index) values at day 3 and 7 post-injury.

In addition, to better dissect the effect of monomeric and toxic a-syn after ischemia, *in vitro* oxygen glucose depreviation was performed in brain microvascular endothelial cells in the absence or presence of a-syn supplemented during ischemia or during reperfusion phase. To further gain deeper molecular insight into how ischemia-reperfusion condition modify α-syn structure, aggregation of the monomeric protein was performed by modifying the pH of buffer solutions *in vitro*. Briefly, monomeric α-syn was aggregated at acidic pH, to mimic the environment during the ischemic episode of stroke injury followed by co-incubation of the aggregates or fibrils with monomeric α-syn in

physiologic buffer to simulate the recovery of pH upon reperfusion. In addition, we studied the effect of candidate therapeutic compounds such as Clusterin and doxycycline in our *in vitro* non cellular model of ischemia- induced-α-syn aggregation.

3. MATERIAL AND METHODS

3.1 Animals

The experiments and animal care procedures were conducted in strict compliance with institutional guidelines and in accordance with national regulations (Legislative Decree No. 26/2014; authorization No. 383/2021-PR, protocol 9F5F5.194 of the Italian Ministry of Health). The personnel involved in conducting the experiments were authorized under the Mario Negri Institutional Regulations and Policies (Quality Management System Certificate—UNI EN ISO 9001:2008, Reg. No. 6121) and adhered to international regulations, including the EEC Council Directive 2010/63/EU (December 12, 1987) and the Guide for the Care and Use of Laboratory Animals issued by the U.S. National Research Council (Eighth Edition, 2011). All animal experiments received prior approval from the Animal Care Unit of the "Mario Negri" Institute and Ministry of Health.

The mice were housed in a Specific Pathogen-Free (SPF) facility under controlled environmental conditions, maintaining a constant temperature of 21±1°C and relative humidity of 60%, with a regulated light/dark cycle (7:00 AM – 7:00 PM). Food and water were available *ad libitum* for at least one week before any experimental procedure. Following surgical interventions, the animals were housed under the same environmental conditions for 48 hours to ensure post-operative recovery. In this study, C57BL/6RCC (wild type) and C57BL/6S (α-syn null) mice, aged between 9 and 12 weeks, were selected. The C57BL/6S mice represent a distinct subpopulation of inbred C57BL/6J mice characterized by a spontaneous deletion of the SNCA (Synuclein Alpha) and Mnrn1 (Multimerin 1) gene locus.

3.2 tMCAo (transient ischemia) model

The induction of ischemia was performed using transient middle cerebral artery occlusion (tMCAo). Anesthesia was induced by inhalation of 3% isoflurane in a gaseous mixture of nitrous oxide and oxygen (N_2O/O_2, 70%/30%) and maintained at 1.5% isoflurane in the same mixture throughout the procedure. During surgery, the animal was placed in a supine position on a thermostatically controlled surgical bed (LSI-Letica, Spain) equipped with a rectal probe to monitor and maintain body temperature at 37±0.5 °C. The surgical site was disinfected with a 4% chlorhexidine solution, and a 1-cm midline incision was made on the ventral surface of the neck. Using a dissecting microscope (Seto, Japan), the right common carotid artery (CCA) was carefully isolated and ligated proximally to the bifurcation between the internal carotid artery (ICA) and the external carotid artery (ECA). Distal to the ligation site, an arteriotomy was performed to allow the insertion of a silicone-coated filament (size 7–0; diameter 0.06–0.09 mm; length 20 mm; coated diameter 0.23 mm; coating length 10±1 mm, Doccol Corporation, Redlands, California, USA) into the ICA. The filament was advanced

cranially until it occluded the origin of the middle cerebral artery (MCA) (Figure 8). Given that the diameter of the MCA is smaller than that of the anterior cerebral artery, only the former was effectively blocked by the filament. The occlusion time for the MCA was set at 30 minutes. During the occlusion period, the animal was allowed to awaken from anesthesia to assess the presence of intra-ischemic deficits, which served as inclusion criteria for the study. After 30 minutes, the animal was repositioned on the surgical table and re-anesthetized to restore cerebral blood flow by gently withdrawing the filament and closing the arteriotomy with a suture. Analgesia was provided through the local application of EMLA cream (2.5% lidocaine + 2.5% prilocaine). The established reperfusion period was 48 hours. A mortality rate of 20% was consistent with the expected outcomes for this experimental model.

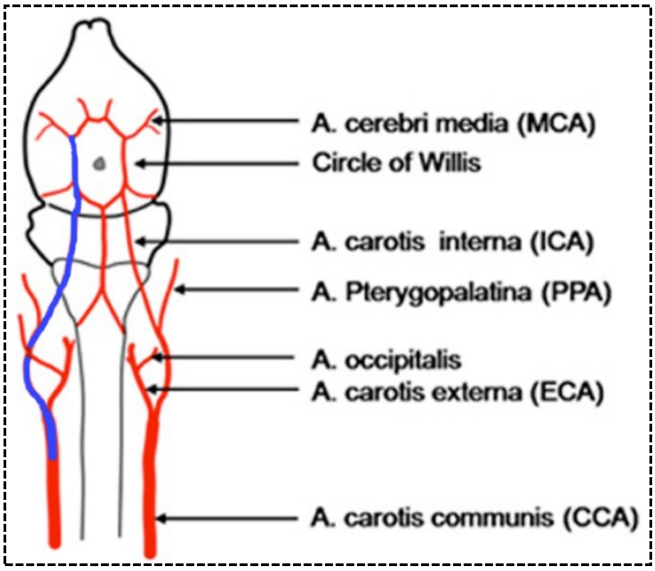


Figure 8. Schematic representation of the murine cerebral vasculature, viewed from a ventral perspective. The blue line indicates the position of the silicone-coated filament in the tMCAo.

3.3 Inclusion/exclusion criteria

Mice were included in the study if transient cerebral ischemia was successfully induced, meaning the filament was correctly positioned at the origin of the middle cerebral artery (MCA). To verify the proper execution of the surgical procedure, animals were monitored during the intra-ischemic period and included in the study if they exhibited at least three of the following neurological deficits:

- An elliptical-shaped eyelid fissure (rather than the normal circular shape)
- One or both ears extended laterally
- Asymmetrical body curvature toward the ischemic side
- Limbs extended laterally and misaligned with the body

Mice were excluded if:

1. they died during MCA surgery

2. Major experimental protocol violations: errors or surgical complications (eg, major arterial or venous hemorrhage, section of the vagus nerve, carotid artery dissection, filament entrapment or displacement) during MCA occlusion procedure; errors in ischemia time.

3.4 Health monitoring

Animals were observed at 24 hours after surgery, before the behavioural test. A predefined Health Report model was used (available at https://figshare.com, DOI: 10.6084/m9.figshare.13031861), following IMPROVE guidelines [127]. Animals showing signs of moderate stress, as reported during Health Monitoring, were given buprenorphine subcutaneously at 0.05-0.1 mg/kg every 8-12 hours. No animals showed signs of severe suffering that would require euthanasia before the end of the experiment.

3.5 Behavioral deficits

9 days after tMCAo each mouse underwent neuroscore evaluation for assessment of sensorimotor deficits [128]. Scores ranged from 0 (healthy) to 56 (worst performance) combining general and focal deficits. The general deficits describe the general well-being of the mouse with a score between 0 and 28. This score includes information on the physical appearance of the mouse, i.e.: fur (0-2), ears (0-2), eyes (0-4), posture (0-4), spontaneous activity (0-4) and presence of epileptic seizures (0-12). Focal deficits describe neurological damage with a score between 0 and 28 and were evaluated through observations on body symmetry (0-4), gait (0-4), ability to climb a 45° inclined plane (0-4), circling behaviour (0-4), forelimb symmetry (0-4), compulsory circling (0-4) and whisker response (0-4) (Figure 9). All mice included in the study that failed to reach the experimental endpoint were given the worst neurological score.

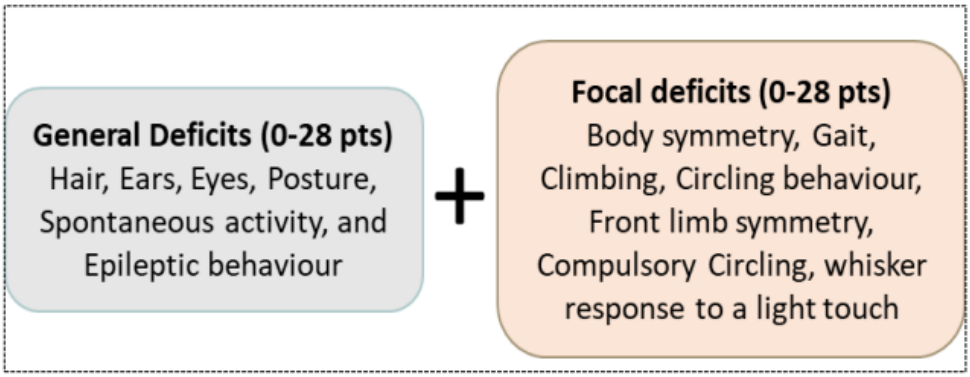


Figure 9. The De Simoni neuroscore.

3.6 Elevated Plus Maze (EPM)

The elevated plus maze was used to evaluate anxiety-like behaviour in a new environment as a measure of cognitive deficit following 28 days of tMCAo and Wt. The maze consists of two opposing open arms (50 cm × 10 cm), an open platform (10 cm × 10 cm) in the center, and two opposing closed arms (50 cm × 10 cm, Figure 10. The maze was elevated 50 cm from the floor. At the beginning of the test, the mice were placed on the central platform facing one of the open arms. The cumulative time spent in the open and closed arms was measured during a 5 min period. The maze was cleaned with 70% ethanol between each test. Videos were recorded and analyzed using Noldus Etho Vision XT video tracking software.



Figure 10. Schematic diagram of EPM test to measure anxiety-like phenotype.

3.7 Barnes Test

The Barnes test assessed spatial learning and memory[129]. The maze consists of a circular platform with multiple holes around its perimeter, only one of which leads to an escape tunnel or a safe area. The test started with habituation trial (day 1) during which the mouse was placed in the centre of the empty arena under a beaker for 30 s, then guided to the escape tunnel over 10–15 s by slowly moving the beaker and allowing 2 min to enter the escape tunnel spontaneously. The mouse was allowed to stay in the safe area for 1 min and then was taken back to its home cage. In the learning phase (days 2–4), mice were placed for 10 s in the centre of the arena and then allowed to explore the arena for at least 2 min to find the escape tunnel (primary latency) and to enter in it (secondary latency). The test phase (day 5) consisted of the removal of the escape tunnel from the maze to assess the primary

latency. The escape was sealed ('false escape') to prevent the mouse from falling through the hole. The ability of the mouse to find the escape within the 2-minute time was recorded.



Figura 11. Schematic diagram of BARNES test to measure learning and spatial memory.

3.8 Brain collection

39 days after tMCAo, mice were anesthetized with Mice were anesthetized with 300 µL of ketamine (150 mg/kg) plus medetomidine (2 mg/kg) intraperitoneally before sacrifice. Mice were transcardially perfused with 30 mL of PBS 0.1 mol/L, pH 7.4, followed by 60 mL of chilled paraformaldehyde (4%) in PBS. The brains were carefully removed from the skull and post-fixed for 6 h at 4°C, then transferred to 30% sucrose in 0.1 mol/L phosphate buffer for 48 h until equilibration. The brains were frozen by immersion in isopentane at – 45°C for 3 min and stored at − 80 ◦C until use.

3.9 Magnetic Resonance Imaging (MRI) acquisition

Image acquisition was performed using a 7T Bruker Biospec scanner (Ettlingen, Germany) equipped with ParaVision 6.01 software and a quadrature cryogenic surface coil functioning as both a transmitter and receiver. Mice were anesthetized with isoflurane (induction at 3–4%, maintenance at 1.5–2%) in a gaseous mixture of 70% N_2O and 30% O_2. Body temperature was maintained at 37°C using a heated water-circulating cradle, and respiratory rate was continuously monitored throughout the procedure. The magnetic resonance imaging study was conducted after 72 hours the ischemic insult using apparent diffusion coefficient (ADC) mapping to quantify the mean extravascular diffusion (D or MD), intravoxel incoherent motion (IVIM) to quantify the perfusion fraction (f) and intravascular diffusion (D*), and T2-weighted imaging (T2WI) to determine lesion size. After 7 days the onset of ischemia, a follow-up MRI was conducted using T2-weighted imaging (T2WI) to assess cerebral remodelling and diffusion tensor imaging (DTI) to evaluate white matter (WM) damage and

investigate differences between the mouse models in their response and recovery following ischemic injury.

3.10 Diffusion-Weighted Imaging (DWI/IVIM)

Echo-planar images (EPI) were acquired (TR/TE = 3000/60 ms, resolution = 0.2 × 0.2 mm², field of view (FOV) = 15 × 15 mm², acquisition matrix = 76 × 76, slice thickness = 0.5 mm) to generate maps of the apparent diffusion coefficient (ADC), pseudo-diffusion intravascular component (D*), and perfusion fraction (f). Diffusion encoding was applied along three orthogonal directions using b-values of 15, 60, 100, 150, 170, 190, 220, 280, 440, 560, 700, 850, and 1000 s/mm². ADC maps were calculated on a pixel-by-pixel basis using a custom MATLAB script with the following model function: $S(b) = SO$

$$S(b) = S0(1 - f)\exp(-bD*) + S0(f)\exp(-bD)$$

Where S(b) represents the signal intensity measured at a given b-value, S0 is the signal intensity in the absence of a diffusion gradient (b = 0). The curve fitting process was carried out in two phases: (1) D and S0(f) were determined by linearizing the model for b-values > 200 s/mm², where the intravascular contribution is negligible; (2) the full relaxation curve was then fitted with D and S0(f) fixed to determine S0(1−f) and D*. Finally, S0 and f were algebraically derived from the calculated S0(f) and S0(1−f) images. Lesion volumes were manually segmented by an experienced operator using the freely available ITK-SNAP software.

3.11 T2-weighted imaging (T2WI)

T2-weighted (T2WI) images were acquired using a 2D Spin Echo (SE) sequence (TR/effective TE = 7500/60 ms, image resolution = 0.1 × 0.1 mm³, FOV = 15 × 15 mm², acquisition matrix = 150 × 150, slice thickness = 0.3 mm). Lesion volumes were manually segmented by an experienced operator using the freely available ITK-SNAP software.

3.12 The ITK-SNAP software

The ITK-SNAP software was designed to provide functions focused on active contour segmentation. It includes tools for 3D image visualization, manual labelling of regions of interest, integration of multiple segmentation outputs, and result processing. The main interface is divided into four panels: three display orthogonal cross-sections of the input image, while the fourth provides a 3D view of the segmented structures (Figure 12).

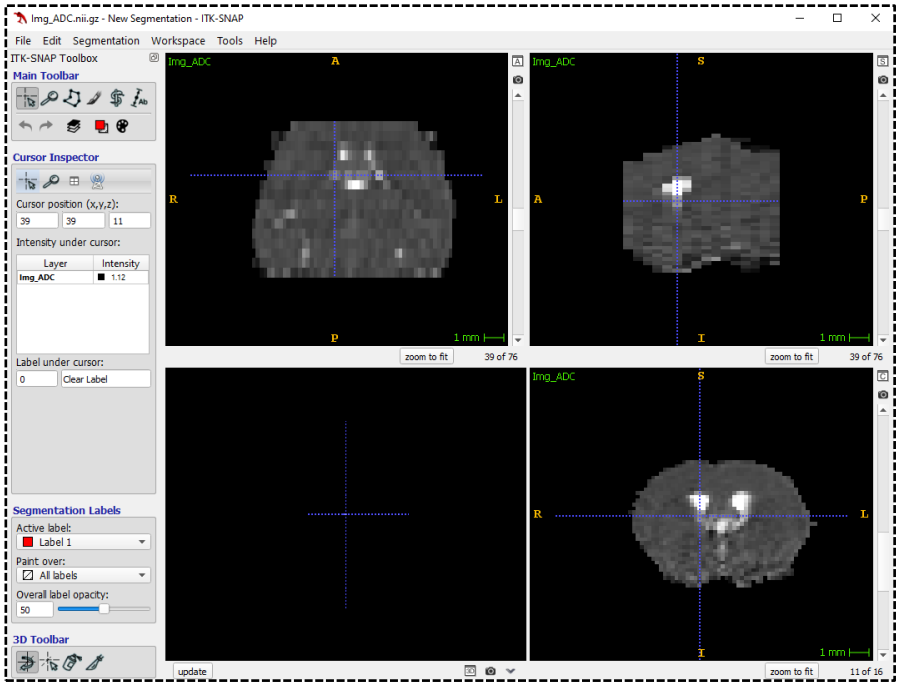


Figure 12. ITK-SNAP software interface.

3.13 *In vitro* ischemia

The ihBMECs cell line was grown in fibronectin-coated ibidi 96-well micro plates to allow adhesion and growth with MCDB (Biowest serum-reduced supplementation medium) supplemented with 0.1% Hydrocortisone and 1% ECG (Endothelial Cell Growth Factor), Fetal Bovine Serum (FBS) 5%, L-Glutamine 1%, Penicillin / Streptomycin 1% at 37 °C in a humidified incubator with 5% CO2. On the day of the experiment, cells in control plate were incubated with low-glucose DMEM with sodium bicarbonate and sodium pyruvate, without L-glutamine and no FBS at 37 °C in a humidified incubator with 5% CO2. In contrast, cells in OGD plate were bathed with DMEM, no glucose, no glutamine, and no FBS in an OGD chamber that was continuously infused with a gas mixture containing 99% nitrogen and <1% oxygen at 37°C for 2h. For reperfusion experiment, half medium was changed to low-glucose DMEM and transferred to a humidified incubator with 5% CO2 for 4h. To analyze the direct effects of α-syn on ihBMECs subjected to OGD-Reperfusion, cells were treated with non-hypoxia preconditioned or hypoxia preconditioned 6ug/ml (0.415uM) endotoxin-free monomers of human recombinant α-syn at the begging of OGD or reperfusion. At the end of experiment, cells from most wells were scrapped off for subsequent RNA extraction (see below).

3.14 Quantitative Real-time-PCR (qRT-PCR)

RNA was extracted from ipsilateral hemispheres using the RNeasy Mini Kit for total RNA extractions (PureLink™ RNA Mini Kit, thermos fisher). Then, 1 µg of total RNA was retro transcribed to cDNA. cDNA (1-5 µL) was amplified with Power SYBR Green (Applied Biosystems) and a mix of forward

and reverse primers (10 μM) and relative gene expression determined with ΔΔCt method. For normalization of quantification, β-actin was used as housekeeping gene.

3.15 Aggregation assay

The aggregation assay was used to assess α-syn aggregation. Monomeric human recombinant α-syn was diluted to a concentration of 50 μM in 0.01 M PBS pH 7.2, with 40 μM thioflavin T (ThT). The solution was transferred to a Corning® 96-well Half-Area Black with Clear Flat Bottom Polystyrene Non-Binding Surface Microplate by adding 75 μL of solution per well, containing a 2-mm zirconium bead (1.5mm). Plates were sealed using Thermowell Sealing Tape (Corning®) to avoid evaporation and incubated on a plate reader (Infinite M200 fluorescence plate reader (TECAN) at 480 nm) at 37 °C under a continuous orbital shaking at 300 rpm. Aggregated α-syn fibrils were recovered from plates and their concentrations (in monomer equivalents) were calculated based on full conversion of monomers. Fibrils were sonicated at 10 μM in 300 μL total volume using a Sonopuls HD2070 microtip sonicator (Bandelin). Then, fibril seeds were added to α-syn monomers and aggregation assays were performed as described above for unseeded assays. Aggregation data were plotted using Amylofit software[130], that include equations describing how proteins forms aggregated structures and to study the effect of various intrinsic and extrinsic factors on the aggregation reaction.

3.16 Statistical analysis

The data were analysed using the GraphPad Prism 8 software (GraphPad Software, La Jolla, CA, USA). Data are presented as mean ± S.D/SEM. Differences were assessed by the Mann-Whitney U test for two groups only or One-way or Two-Way analysis of variance (ANOVA) for grouped data. When the p-value in the ANOVA test indicated statistical significance, the differences were assessed by Sidak's post hoc analysis.

4. RESULTS

In vivo

4.1 Alpha-synuclein deficiency improved mice survival after 30-min of tMCAO

We subjected C56BL/6S α-syn null mice, and C57BL/6JRCC wild-type mice to 30 min of ischemia-reperfusion injury and then evaluated neurological deficits, and survival measures of stroke outcomes. Sensorimotor deficits were assessed 9 days after tMCAo using a composite neuroscore as previously described[131]. Ischemia induced comparable deficits in C57BL/6RCC and C56BL/6S mice 9d after tMCAo (figure 13a). While, 30 days after tMCAo, the survival rate of C56BL/6S α-syn null mice was higher, yet not statistically significant than that of C57BL/6RCC mice (figure 13b), with all the majority of deaths occurring in C57BL/6RCC male mice (4/6) within 3-14d after tMCAo. Both of these findings are consistent with our previous observation that the absence of ischemia-induced α-syn toxicity in null mice confers protection in the post-acute phase of brain ischemia-reperfusion injury.

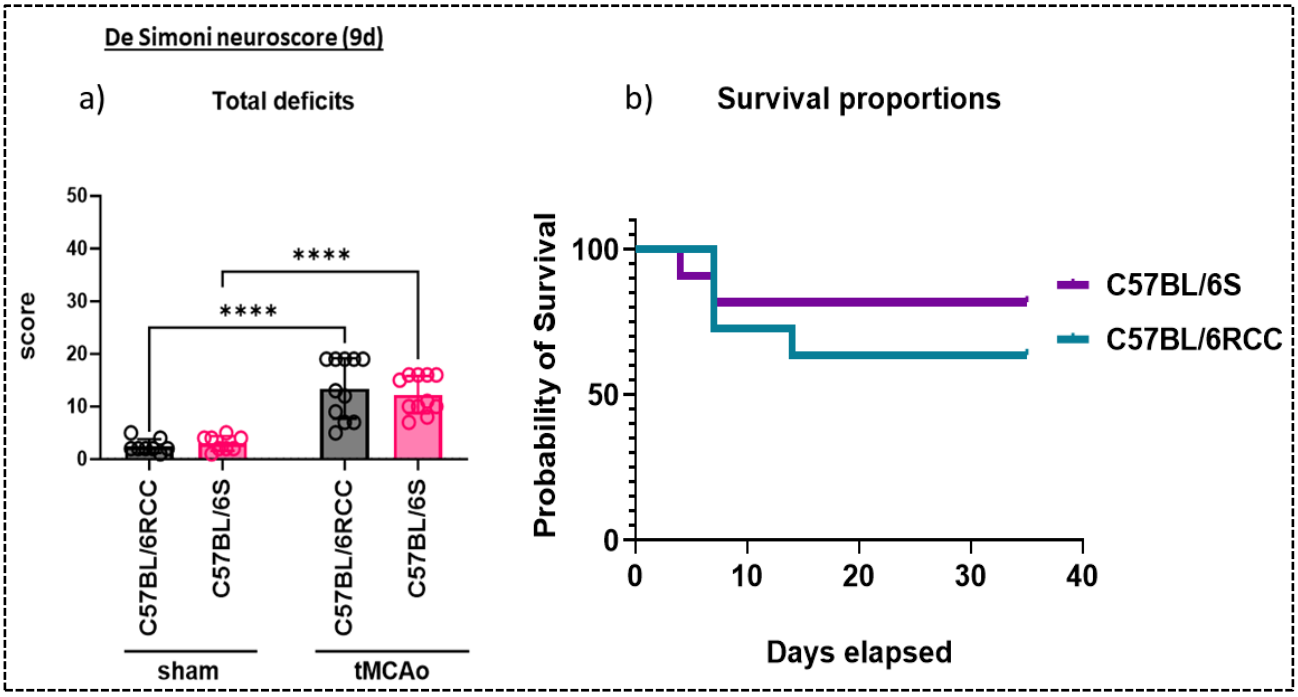


Figure 13. Alpha-synuclein deficiency improves survival after ischemic stroke. a) Sensorimotor deficits assessed by using a composite neurological score 48h after tMCAo (n, Sham =8; tMCAo= 6 for C57BL/6RCC, 8 for C57BL/6S**).** Data are presented as mean ± SD and analyzed by two-way ANOVA followed by Sidak's post-hoc test, *p<0.05, **p<0.01, ***p<0.001, ns= not significant. b) The Kaplan-Meier survival curve shows better survival in C57BL/6S than C57BL/6RCC mice in the days after 30 min tMCAo (Log-rank Mantel-Cox test, p>0.05, n=10for C57BL/6JRCC and 10 for C57BL/6S).

4.2 Alpha-synuclein null mice show increased infarct volume at 3 days but an enhanced recovery at 7 days after tMCAo

To assess the effect of the lack of α-syn in ischemic brain damage during the different phases of tMCAO, we utilized T2 MRI imaging 3 and 7 days after tMCAo. On day 3 α-syn null mice brains exhibited significantly increased infarct volumes compared to wt controls (figure 14a). While at 7 days, both α-syn null and wt tMCAo exhibited a significant reduction in lesion volume (figure 14b) with α-syn null tMCAo mice showing an enhanced recovery of the ischemic lesion at 7 days compared to their initial lesion volume observed at 3 days after stroke (figure 14c).

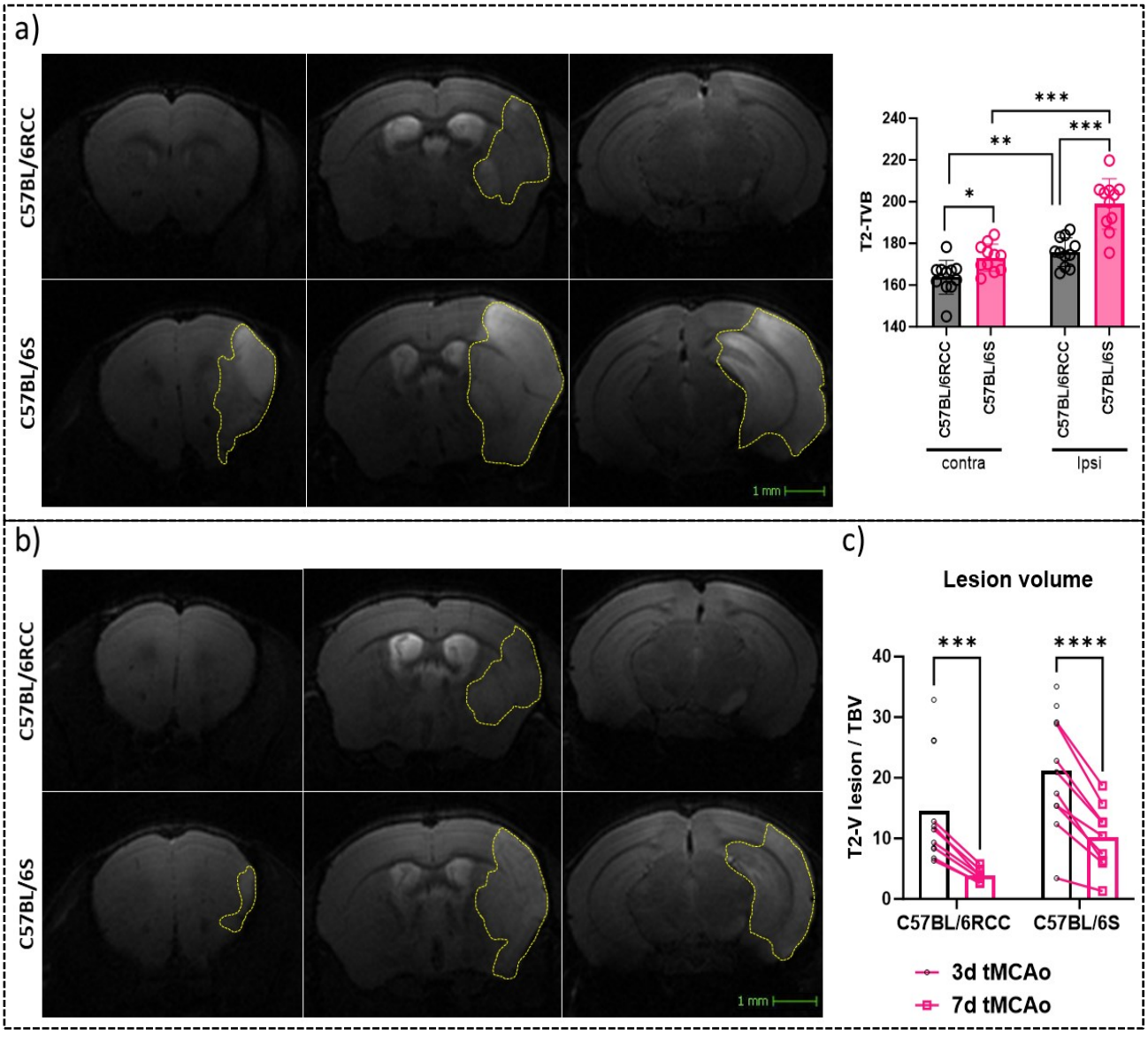
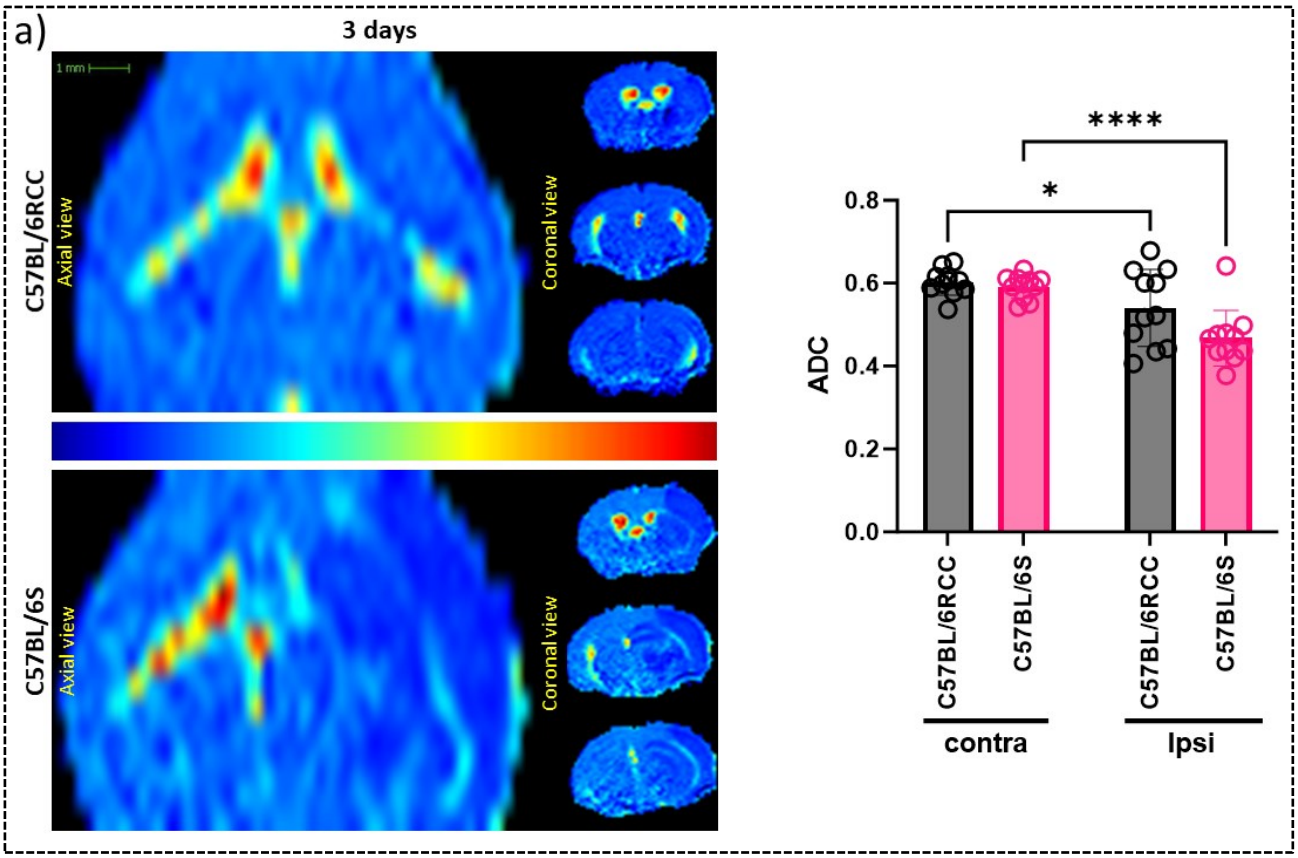


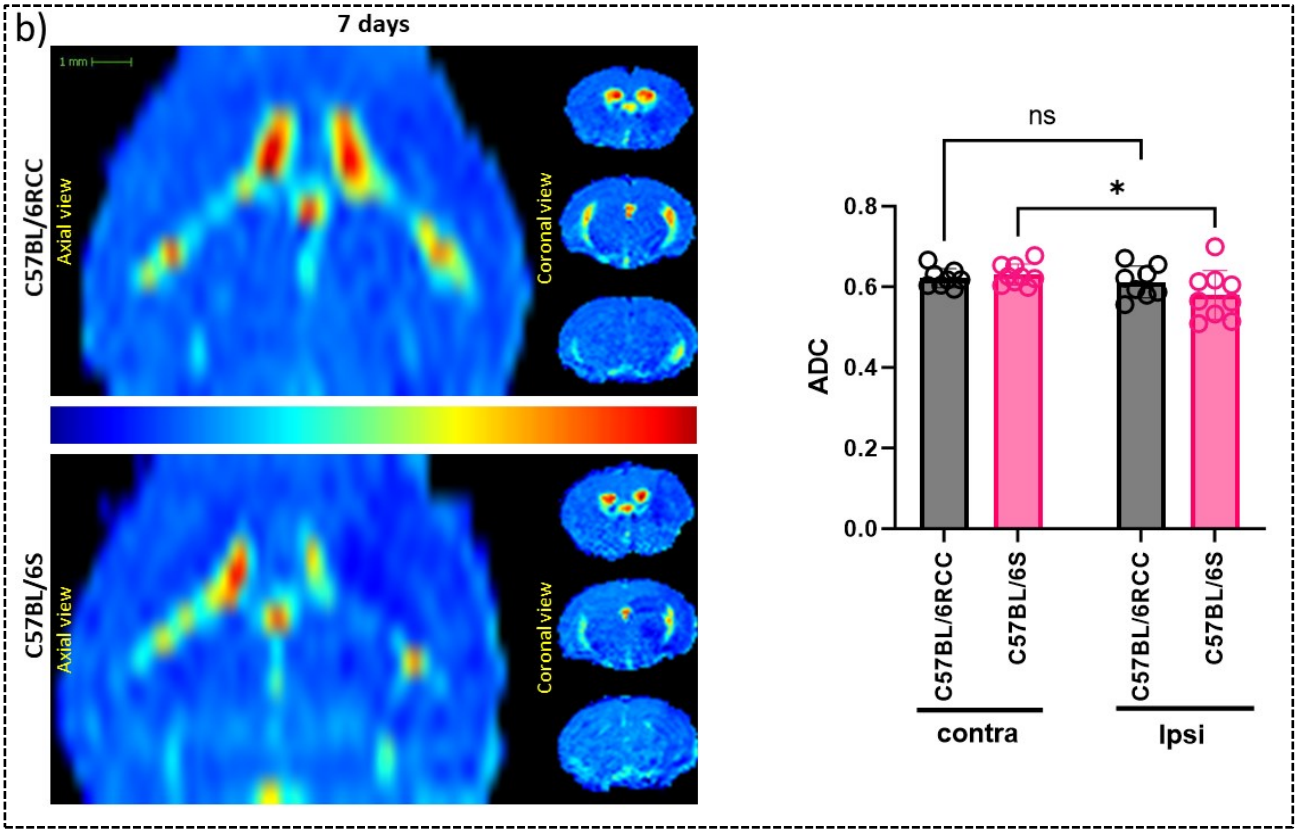
Figure 14. Alpha-synuclein loss leads to bigger brain infarct size acutely but favours a faster recovery. Cranial MRI was used to measure infarct volume at day 3 (a) and day 7 (b) after tMCAO in wild type (C57BL/6RCC) and α-syn null (C57BL/6S) mice (representative T2 images).

Quantification of T2-weighted (T2-V) lesion volume normalized to total brain volume (TBV) in C57BL/6RCC and C57BL/6S mice c) Pink lines connect paired values from individual mice at 3 day (black graphs) and 7 days (pink graphs) after tMCAo. Data are presented as individual values ± SD and analyzed by unpaired T test with Welch's correction in a and b or paired two-way ANOVA. ***p < 0.001, ****p < 0.0001 in c.

4.3 Alpha-synuclein null mice show worsened brain ischemia induced cerebrovascular flow deficit at 3 days after tMCAo, but enhanced recovery after 7 days

Unpublished previous study of ours indicated that the loss of α-syn suppressed the expression of vascular permeability factors 48h after tMCAo in young male α -syn null mice. Hence in this study we tested the hypothesis that this effect could be associated with improved BBB leakage in α-syn null mice. To measure cerebrovascular flow, diffusion weighted magnetic resonance imaging was applied in male and female mice at 3 and 7 days after tMCAo (figure 15). We observed a significant decrease in ADC values in ipsilateral cortex and striatum of α-syn null mice and to a letter extent in wild type RCC mice brains (figure 15a and b). Interestingly, α -syn null mice showed a robust recovery (****p < 0.0001) in ADC values at 7 days despite higher reduction at 3 days after tMCAo (figure 15c).





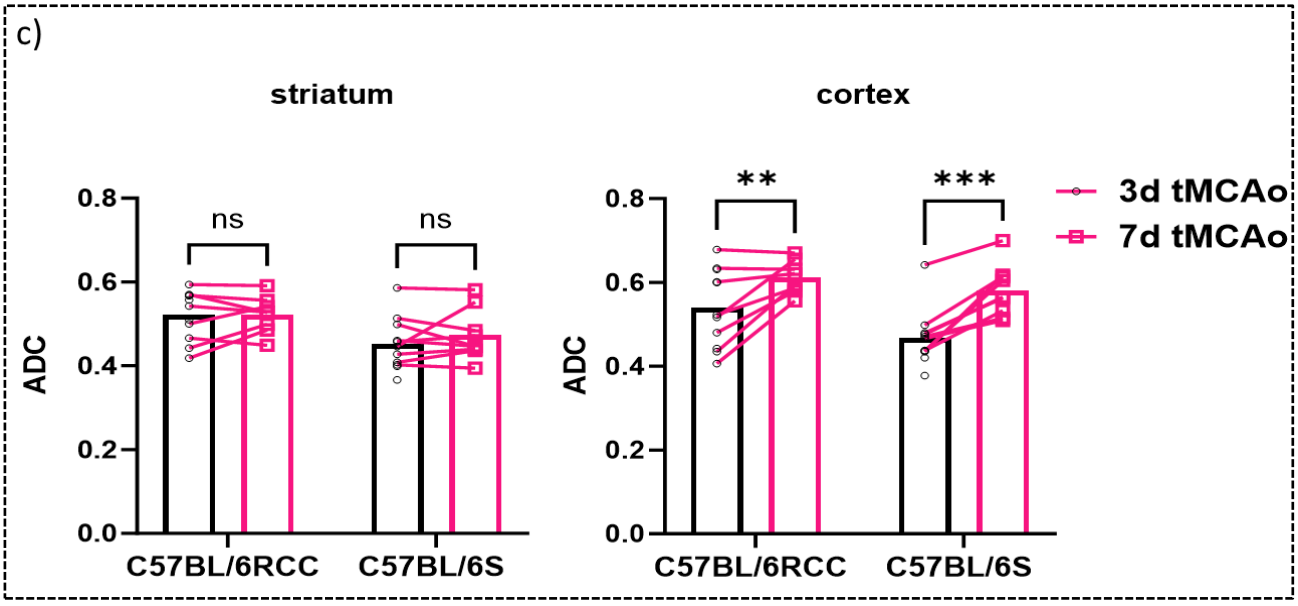
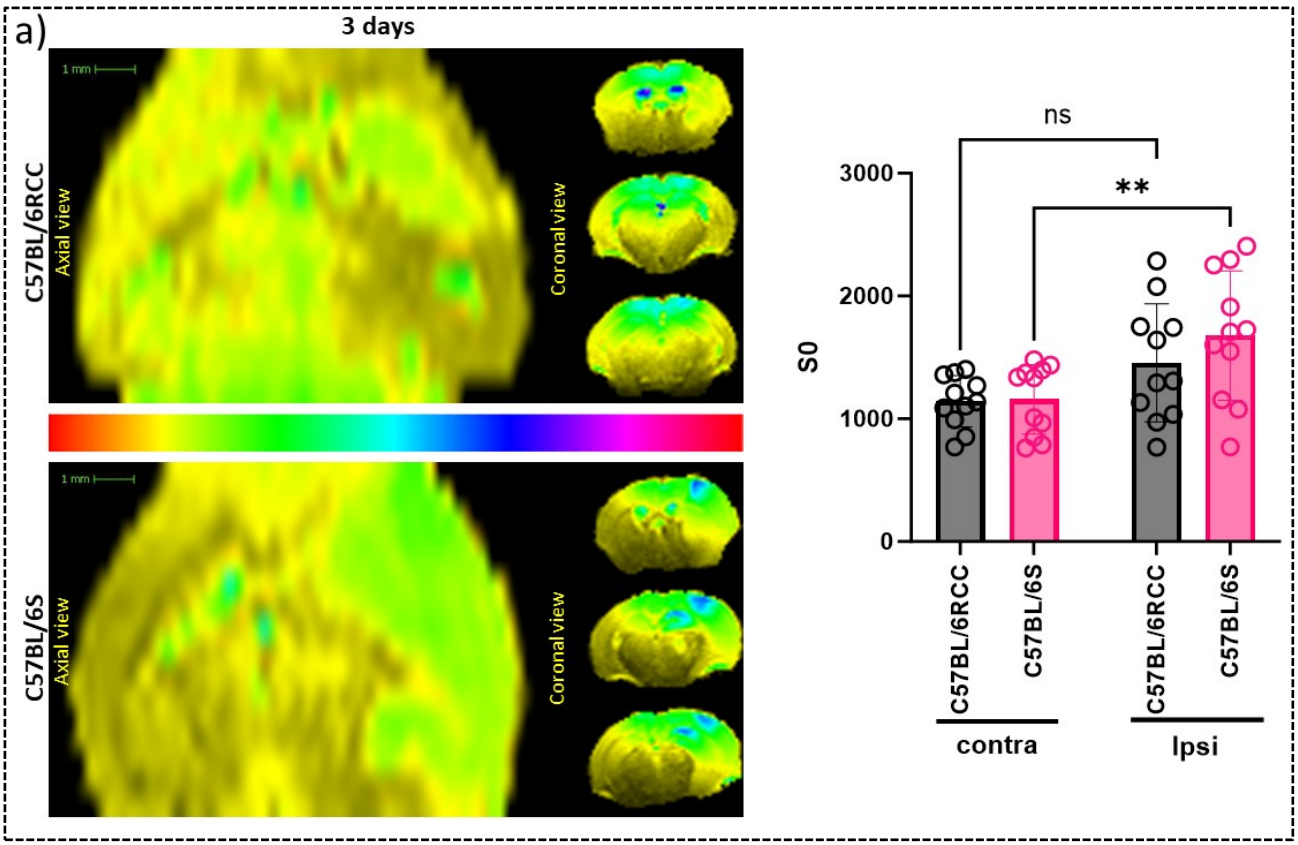


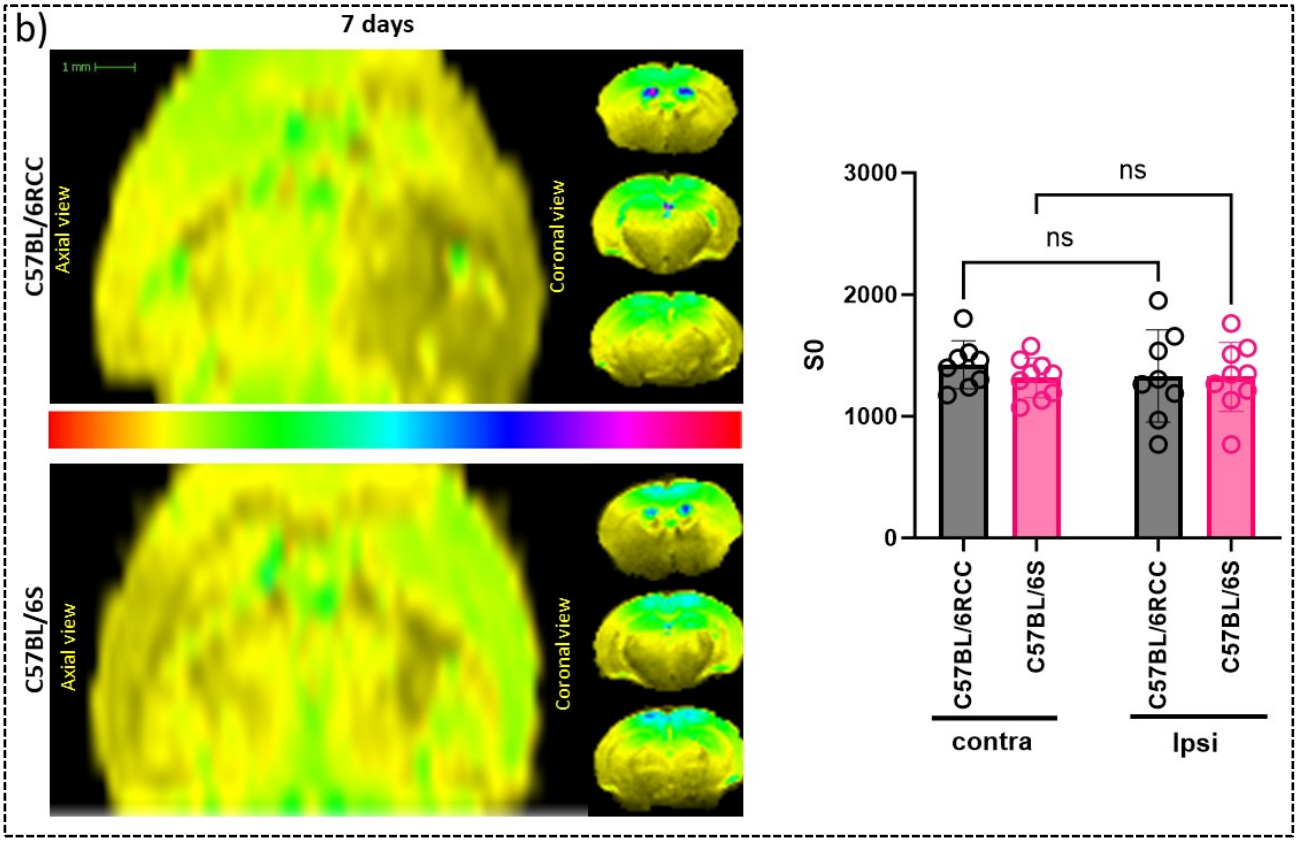
Figure 15. Alpha-synuclein null mice exhibit an enhanced recovery in cerebrovascular flow at 7 days after tMCAo. a) and b) show representative ADC map of wild type (RCC) (above) and null (bottom, a-syn null) mice brains 3 and 7 days after tMCAo in axial (left) and coronal views (right). Graphs show the absolute ADC values in the ipsilateral and contralateral cortex and striatum of each of the tMCAo animals that underwent MRI on day 3 and 7. Images were visualized with *JET* color-coded pixel, dark blue colour means less perfusion, scale bar=1mm. Data are presented as individual values ± SD and analyzed by unpaired t-test with welches correction, *p<0.05, **p<0.01, ***p<0.001 c)

Quantification of ADC in C57BL/6RCC and C57BL/6S mice. Pink lines connect paired values from individual mice at 3 day (black graphs) and 7 days (pink graphs) after tMCAo. Data are presented as mean ± SD and analysed using a paired two-way ANOVA. ***p < 0.001, ****p < 0.0001.

4.4 Alpha-synuclein null mice exhibited increased vasogenic edema at 3 days following tMCAO, but demonstrated accelerated edema resolution by day 7

To measure vasogenic edema (S0), diffusion weighted magnetic resonance imaging was applied in male and female mice at 3 and 7 days after tMCAo (figure 16). Alpha-synuclein null mice showed increased vasogenic edema at 3 and 7 days as measured by S0 value (figure 16a and b). We observed a significant decrease in S0 values in ipsilateral cortex and striatum of α-syn null mice and to a letter extent in wild type RCC mice brains (figure 16c), indicating a faster recovery by the α-syn null mice.





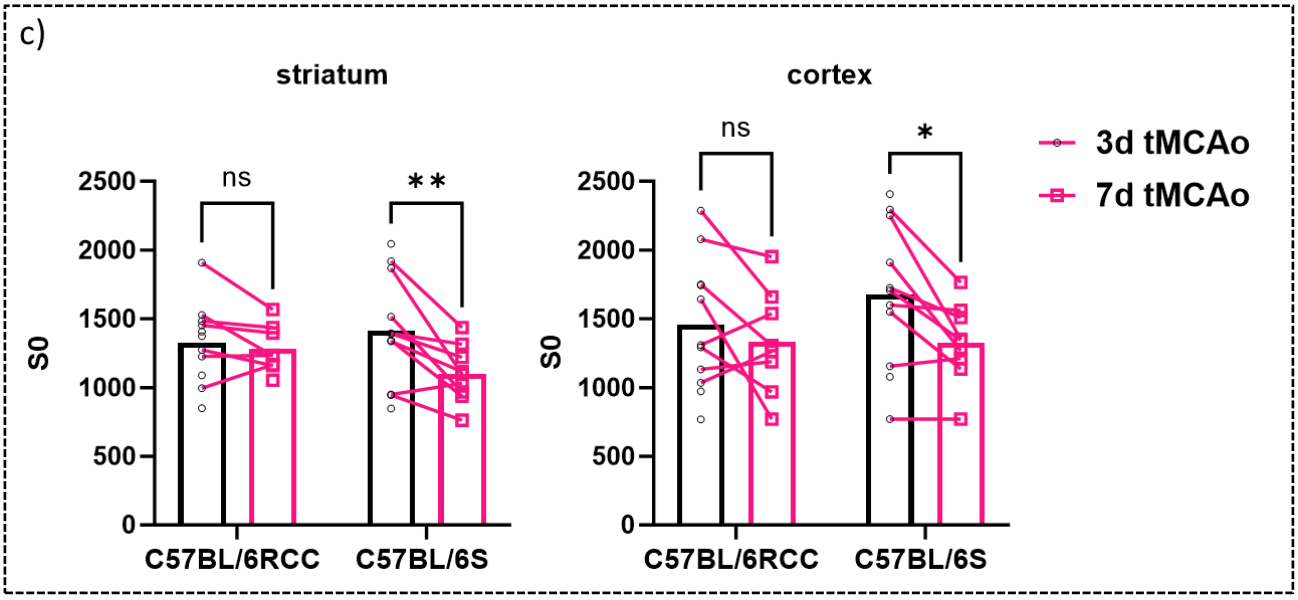


Figure 16. Alpha-synuclein null mice exhibit an enhanced recovery in vasogenic edema at 7 days after tMCAo. a) and b) Representative S0 map of wild type (RCC) (above) and null (bottom, a-syn null) mice brains in axial (left) and coronal views (right). Images were visualized with *HSV* color-coded pixel, green colour means more vasogenic edema, scale bar=1mm. Graphs illustrates the absolute S0 values in the ipsilateral and contralateral cortex and striatum of each of the tMCAo animals that underwent MRI on day 3 and 7. Data are presented as individual values ± SD and

analyzed by unpaired t-test with welches correction, *p<0.05, **p<0.01, ***p<0.001 c) Quantification of S0 in C57BL/6RCC and C57BL/6S mice. Pink lines connect paired values from individual mice at 3 day (black graphs) and 7 days (pink graphs) after tMCAo. Data are presented as mean ± SD and analysed using a paired two-way ANOVA. ***p < 0.001, ****p < 0.0001

4.5 The absence of ischemia induced α-syn toxicity did not attenuate long-term functional and cognitive deficits after tMCAo

Based on our previous study that showed reduced anxiety-like phenotype and improved motor performance in α-syn null ischemic mice 7 days after tMCAo, we extended the use of EPM to understand whether the loss of α-syn influence these phenotypes also at a longer time point (28 days after tMCAo). We observed that both sham controls and tMCAo mice spent more time in closed arms compared to open arms (figure 17a). Interestingly tMCAo mice spent less time in the centre zone compared to sham controls, with statistical significance reached only between sham and tMCAo null mice, which may indicate a reduced explorative behaviour in these mice. However, no difference was observed in overall anxiety score nor in the total distance travelled across the experimental groups (figure 17a). To assess whether ischemia induced α-syn toxicity influence spatial learning and memory in mice after tMCAo, we used Barnes maze and calculated the latency to find a target hole in a circular maze over 3 days (figure 17b). Our data showed that ischemic and sham α-syn null mice initially took longer time to find the target hole, as compared to wild type sham controls (figure 17b). However, α-syn sham mice showed improvement in learning performance starting from the second day of training as evidenced by a decrease in latency (figure 17b). On day 3 of the training, the α-syn null, but not wild type tMCAo mice still took significantly longer time compared to their respective sham controls to find the target hole (figure 17b). During the final probe trial day, wild type, but not α-syn null tMCAo mice took longer time to find the false escape compared to their respective sham controls (Figure 17b). These data suggest that lack of α-syn may influence long-term functional and cognitive deficits after tMCAo.

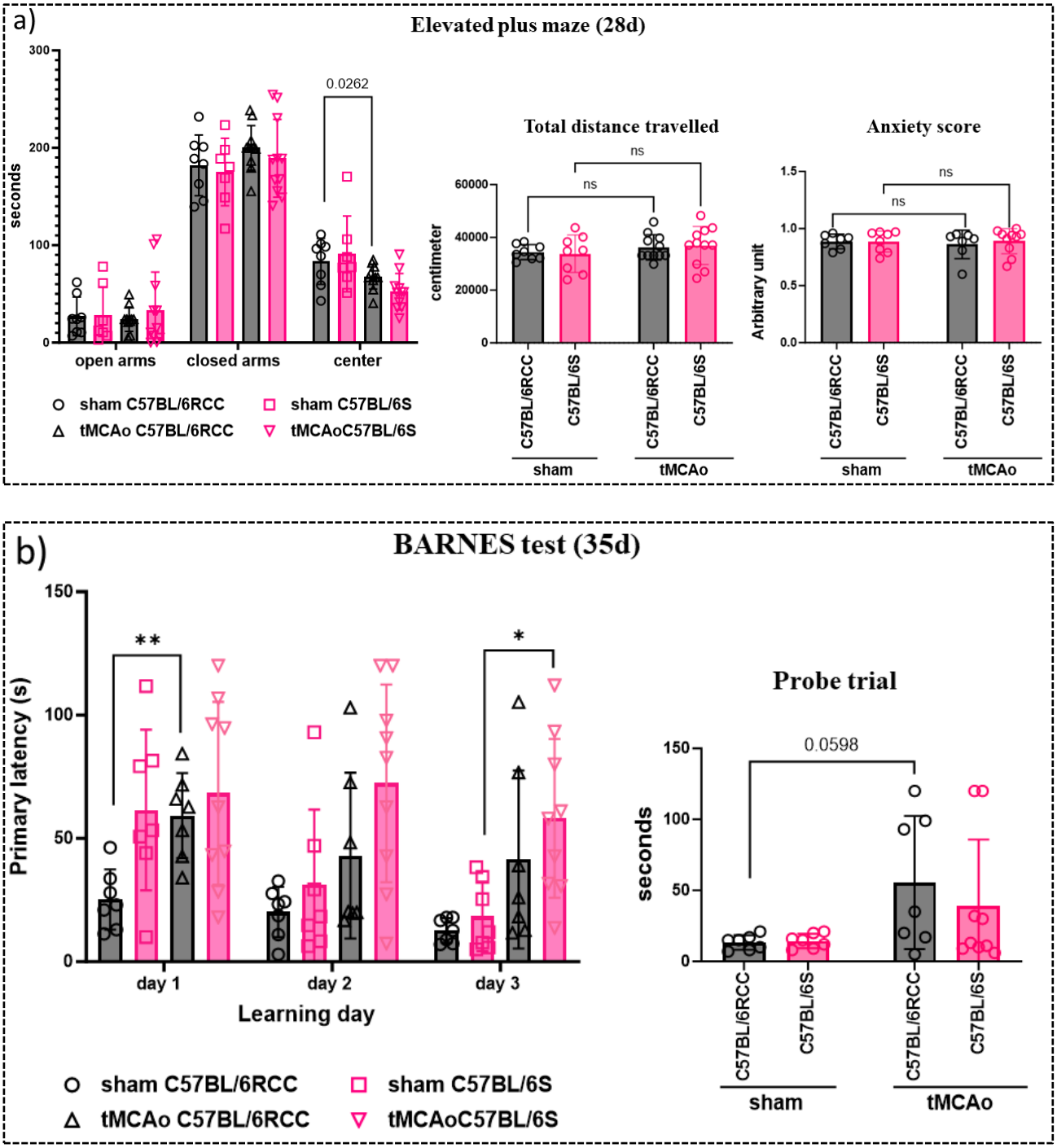


Figure 17. Performance of α-syn null and wild type mice in EPM and Barnes maze a month after sham/tMCAO surgery. a) The time spent and the total distance traveled in closed arms, open arms and centre zone (measured in seconds), and in the open arms, closed arms, and center measured in centimeters assessed using EPM 28days after tMCAo (○=for wt sham, Δ= for wt tMCAo, ▼ = for null tMCAo, □= null sham). Anxiety score is obtained comparing time spent in open arms and time spent in closed arms. b) mice were tested for primary latency during the acquisition days (d1-d3) and during probe trial (d4) in the Barnes maze 1-month after tMCAo. Data are presented as mean ± SD

and analyzed by two-way ANOVA followed by Sidak's post-hoc test, *p<0.05, **p<0.01, ***p<0.001, ns= not significant.

In vitro

4.6 Extracellular ischemia altered α-syn further exacerbates I/R injury while monomeric α -syn reduced inflammation in microvascular endothelial cells

Our previous unpublished data that showed hypoxia altered a-syn further increased the induction of *ICAM-1 in vitro* model of oxygen-glucose deprivation and reoxygenation (OGD-R) on human microvascular endothelial cells. To further understand the effect of monomeric unaltered a-syn in endothelial injury that follows OGD, we performed an *in vitro* experiment where *ICAM-1 expression* was compared in ischemic cells in the presence or absence of recombinant monomeric α-syn added during the reoxygenation phase (in dark turquoise) or at the beginning of OGD (in pink) (figure 18a). Our data showed that *ICAM*-1 expression was increased after treatment with recombinant human monomeric α-syn supplemented during the OGD (figure 18b). Interestingly, the addition of the protein at the beginning of the reperfusion suppressed the increased expression of *ICAM-1,* suggesting the role of ischemia altered α-syn in mediating endothelial injury while a protective role for monomeric α-syn (fig 18b).

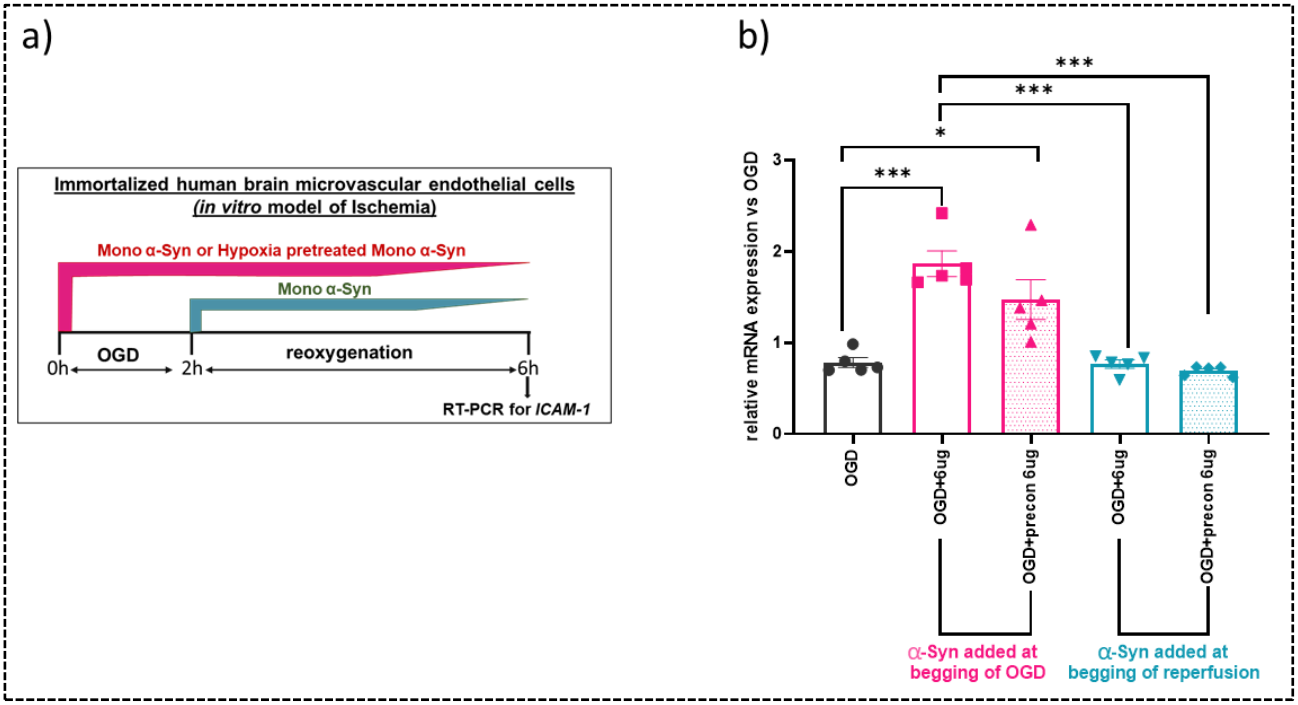


Figure 18. Hypoxia altered monomeric a-syn is detrimental to microvascular endothelium. a) Schematic diagram of OGD followed by reoxygenation experiment in ECs in the presence or absence of recombinant monomeric α-Syn added during the reoxygenation phase (in dark turquoise) or at the beginning of OGD (in pink). b) show *ICAM-1* mRNA in ischemic ECs. Data are presented as

individual values ± S.D. and analyzed by multiple comparisons two-way ANOVA followed by Sidak's post hoc test, *p < 0.05, **p < 0.01, ***p < 0.001

4.7 Hypoxia promotes the aggregation of monomeric α-syn in non-cellular condition

We compared the aggregation kinetics of hypoxia and normoxia preconditioned recombinant human monomeric α-syn, by monitoring the increase in ThT fluorescence intensity over time. We observed that hypoxia preconditioned of α-syn aggregates faster with higher amplitude compared to normoxia preconditioned one (figure 19a). Investigation of the secondary structures of the aggregates using far-UV (190–260 nm) circular dichroism (CD) showed that the spectra of hypoxia preconditioned α-syn aggregates show a higher contribution from a prominent negative CD band at 200 nm compared to the normoxic α-syn aggregates (figure 19b), suggesting the presence of more compact and well-defined β-sheet rich amyloid fibrils in hypoxic condition. Overall, our preliminary data suggest that α-syn is prone to aggregate in hypoxic condition such as in ischemic event.

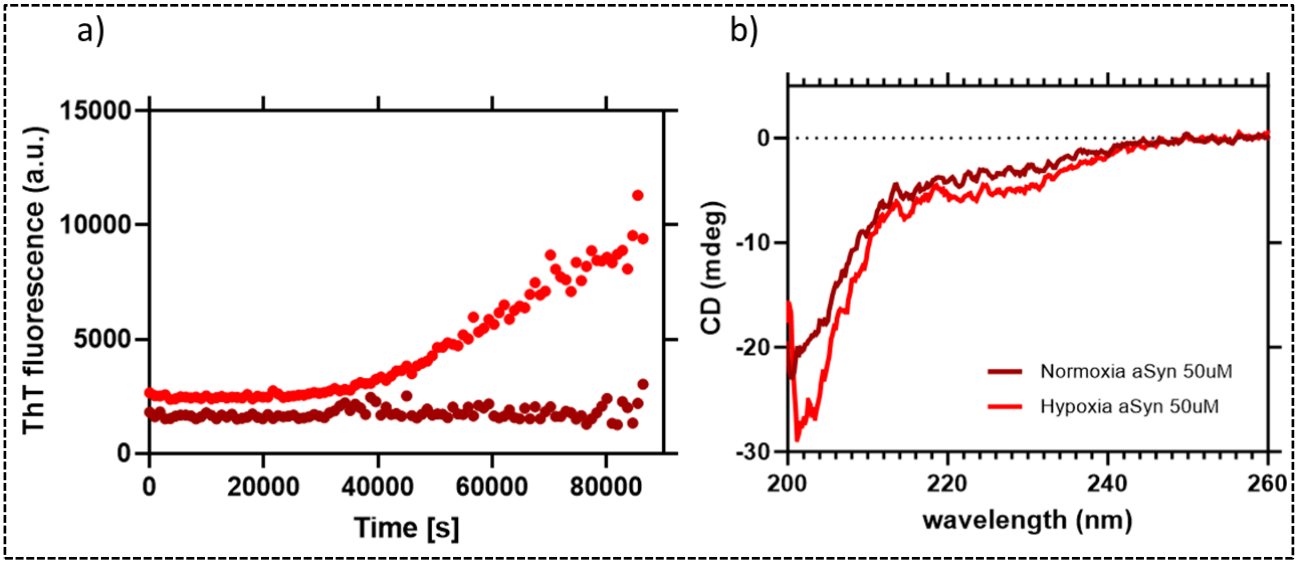


Figure 19. *In vitro* aggregation of α-syn. a) Aggregation of 50 µM monomeric Alpha-synuclein in Hypoxia and Normoxia conditions, compared by monitoring the increase in ThT fluorescence over time. Data are mean values of multiple reads per well per time. b) Circular dichroism spectra of α-syn and spectral deconvolution. One Gaussian at 200nm is fitted for random beta sheets.

4.8 Alteration of pH of buffer solutions mimics *in vivo* ischemia induced α-syn pathology

We first performed aggregation assay in PBS buffer by artificially reducing the pH to 5 to simulate the ischemia induced acidosis. In line with our preliminary data in figure 19, our data showed that

acidic environment enhanced the aggregation of α-syn at 25μM and 50μM concentration and the formation of compact β-sheet structures compared to control condition (Figure 20).

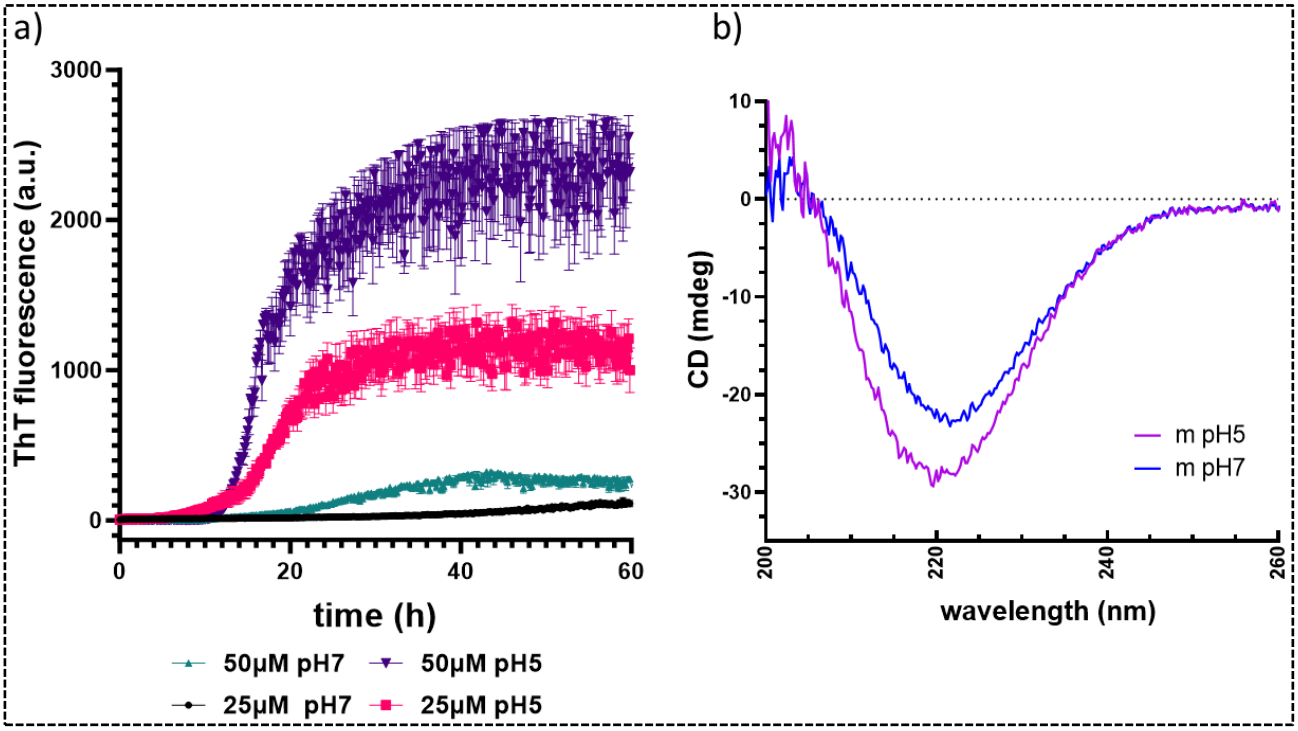


Figure 20. *In vitro* aggregation of α-syn in a buffer solution with pH 5 and pH 7. a) Aggregation of 25 μM and 50 μM of recombinant human monomeric α-syn in acidic and neutral pH was compared by monitoring the increase in ThT fluorescence over time. Data are mean values of multiple reads per well per time. b) UV CD spectra of α-syn fibrils formed in (a) and was ultracentrifuged and resuspended in 20mM PB buffer. The measurements were carried out in room temperature (25 °C).

4.9 Clusterin and Doxycycline exert complete inhibition of α-syn self-aggregation in acidic and physiologic pH respectively in non-cellular condition

We tested the effect of Clusterin and doxycycline, compounds that have been previously described to inhibit protein aggregation [132,133]. Our results showed that Clusterin specifically inhibits the aggregation of monomeric α-syn in acidic pH with no or minimal effect in neutral pH as evidenced by a change in ThT fluorescence (figure 21b). Conversely, Doxycyline inhibited the aggregation of α-syn completely at neutral pH (figure 21a) in line with previous studies [132].

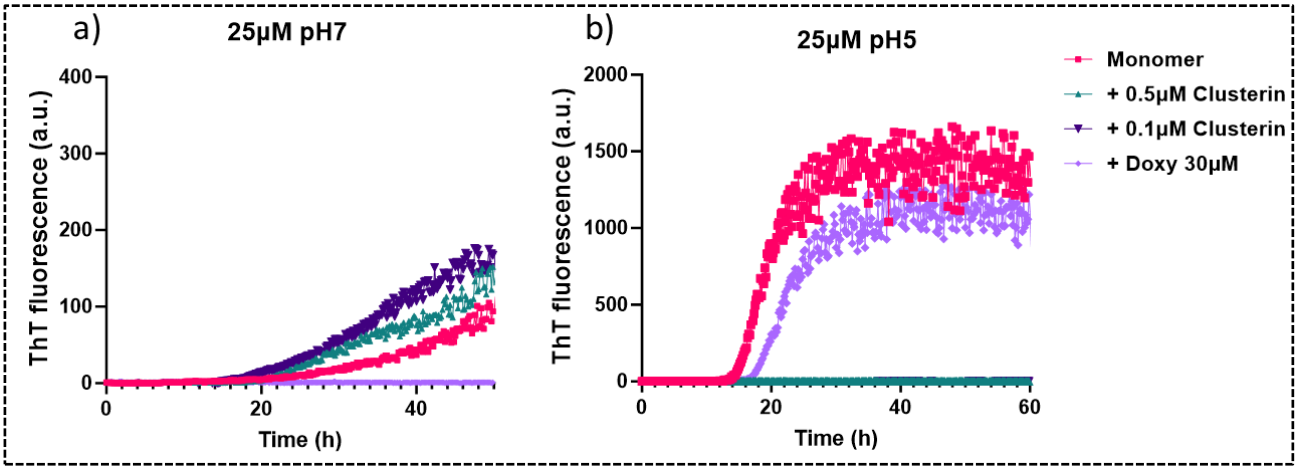


Figure 21. Clusterin and doxycycline interfere with α-syn aggregation at pH 5 and pH 7 respectively. Aggregation of 25 µM of recombinant human monomeric α-syn in neutral pH (a) and acidic pH (b) alone or in the presence of recombinant human Clusterin (0.1 and 0.5µM) or Doxycyline 30µM was compared by monitoring the increase in ThT fluorescence over time. Data are mean values of multiple reads per well per time.

4.10 Alpha-synuclein fibrils produced at acidic pH exhibit superior seeding of monomeric protein

Previous studies reported a decrease in brain intra and extracellular pH due to ischemia-induced acidosis followed by a recovery to a neutral pH upon reperfusion [134]. To better simulate the dynamic pH changes that occur during ischemia-reperfusion injury and their effect on α-syn aggregation, we performed co-aggregation of α-syn fibrils or seeds, which were formed at either acidic (ischemia condition) or neutral pH (disease unrelated condition), with monomeric α-syn in buffers of either matching or differing pH conditions (figure 22). We performed low seeding experiment with 0.1 and 1% of α-syn fibrils in a total protein concentration of 25uM in the presence or absence of Clusterin and doxycycline (figure 22b). Fibrils from aggregation in acidic condition (S5) show a high capacity in seeding monomeric α-syn at pH 7 (reperfusion condition) compared to seeds produced at physiology pH (S7). Global fitting analysis shows that α-syn aggregation is dominated by secondary nucleation in ischemia mimicking and reperfusion conditions. The significant reduction of lag time upon addition of 0.1% seeds and global fitting analysis confirms this finding.

Interestingly, in reperfusion conditions, the seeds produced at ph5 (acidosis) and co-aggregation with monomeric a-syn occuring at pH7, 0.1µM Clusterin delayed a-syn aggregation (figure 22c). On the other hand, incubation with 30µM doxycycline did not affect α-syn aggregation in reperfusion condition, suggesting a superior inhibition by Clusterin of cross seeding of α-syn in this condition.

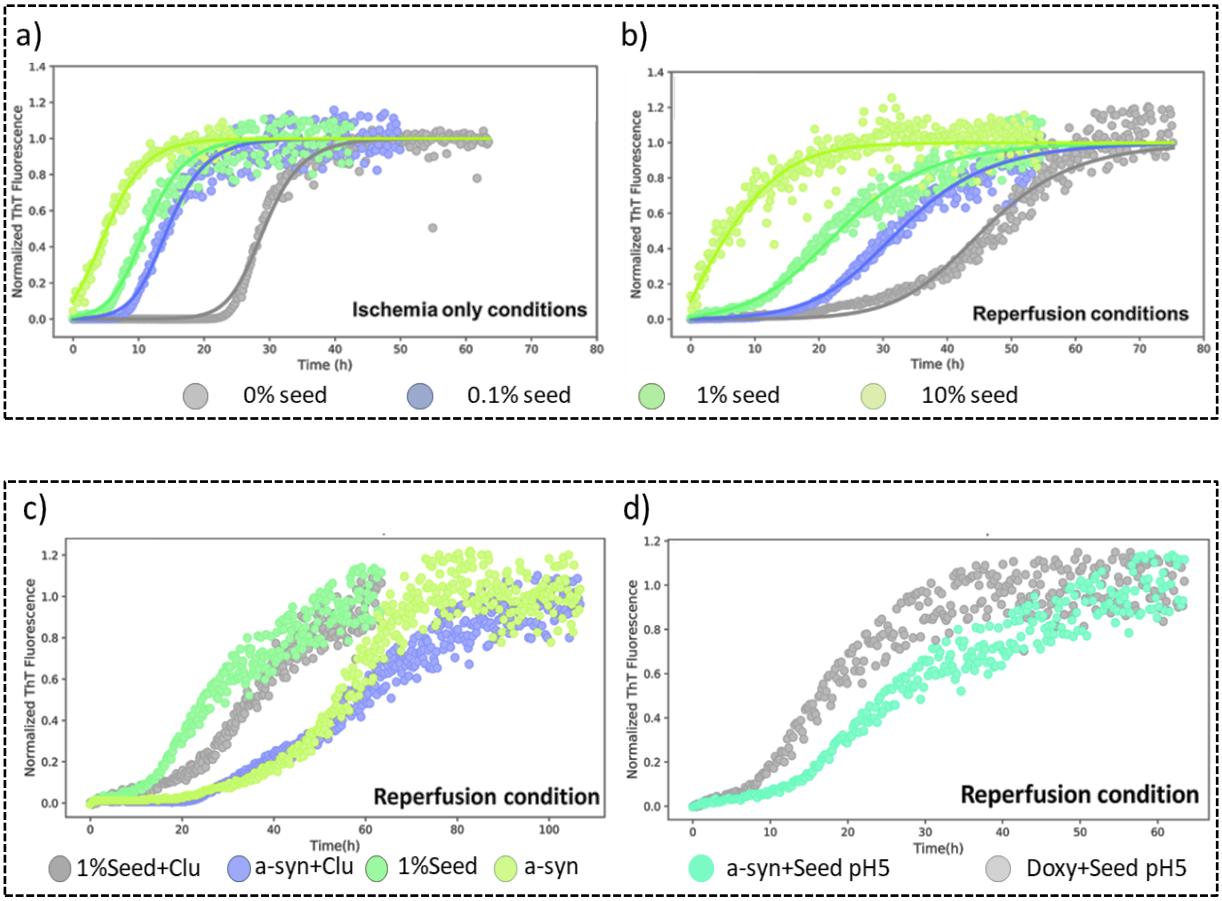


Figure 22. Growth of α-syn fibrils at very low seed concentrations (0.1% and 1% of seeds produced in acidic pH in PBS buffer (pH pH 5 (ischemia only condition, a) or 7 (reperfusion condition, b) at 37 °C, shaking conditions) in a total protein concentration of 25uM. C and d show seeding experiment only in reperfusion condition in the presence of 0.1µM Clusterin (c) and 30µM doxycycline (d). Data are mean values of multiple reads per well per time.

5. Discussion

This thesis work shows that ischemic stroke induces α-synuclein pathology that may impact on brain hemodynamic and stroke recovery. Our data support the hypothesis that the aggregation of α-syn is a secondary event to ischemic onset, affecting the functionality of blood vessels and absorption of cerebral vasogenic edema. Based on previous data of our lab that showed that the lack of α-syn suppressed the expression of vascular permeability factors at 48h after tMCAo, we subjected ischemic wild-type and null mice to neuroimaging by MRI. Our data showed that 3 days after brain ischemia α-syn null mice exhibited significant higher brain infarct size, impaired blood flow and worse vasogenic edema compared to wt controls. This result suggests that α-syn null mice might have impaired collateral blood flow, which determines the extent of initial brain damage due to an intrinsic baseline difference in brain development, as previous published study have shown. Moreover, we can hypothesize that endogenous α-syn may be required for protective neurovascular inflammatory response that may impact the progression of ischemia reperfusion injury. However, we acknowledge that α-syn null mice are also deficient for multimerin-1 protein that is basally expressed in vascular endothelial cells and platelets, overall making the null model prone to develop a bigger lesion. Interestingly at 7 days after stroke, α-syn null mice showed similar MRI parameters of hemodynamic with wild-type mice, implying an enhanced recovery of blood flow and absorption of vasogenic edema. This is in line with improved survival observed at long term in α-syn null mice. However, this is not enough to improve their performance at cognitive tests that may be ascribed to the complete absence of α-syn which is needed for brain plasticity. Indeed our in vitro data demonstrated that ischemic microvascular cells exposed to monomeric α-syn could reduce inflammatory profile by decreasing overexpression of *ICAM-1*.

To summarize the data obtained by our in vivo and in vitro model of ischemia we can hypothesize that ischemia induces α-syn pathology in time dependent manner which in turn contributes to brain injury. On the other hand, the lack of α-syn may influence the initial ischemic brain damage and recovery. Due to inner limitations of using a null mouse model -which is devoid of α-syn through animal whole life-we cannot dissect the specific contribution of physiological monomeric α-syn (protective) and pathological aggregated α-syn (toxic). As such in order to specifically study the mechanism by which ischemia induces aggregated α-syn we moved to an in vitro non-cellular model. Namely, we developed a model of α-syn aggregation in ischemia-reperfusion mimicking condition by reducing the pH of the buffer containing α-syn monomers. This mirrors the acidic environment that occurs in the ischemic territory after hypoxia/ischemia. subsequently, to mimic reperfusion condition, α-syn aggregates formed in acidic environment were co-aggregated with monomeric α-syn in a buffer at physiologic pH. Using our model, we observed that acidic environment induces faster

and higher aggregation of α-syn characterized by a compact b-sheet structure compared to α-syn aggregates formed in physiologic pH. Moreover α-syn fibrils formed during ischemic condition showed a higher seeding capacity evidenced by faster aggregation kinetics compared to fibrils formed in physiologic pH.

Since our data indicates that α-syn aggregation could be a pharmacological target in ischemic stroke, we tested in our in vitro model two compounds known to interfere with aggregation of amyloidogenic protein like α-syn. Namely, we applied Doxycycline and Clusterin in both seeded and unseeded conditions of α-syn aggregation. Interestingly we observed a complete inhibition of monomeric α-syn self-aggregation in the presence of Clusterin in acidic conditions and Doxycycline in physiologic pH. This latter is in line with previous studies [125], while for Clusterin our data represent a new piece of information supporting future development of the compounds in more complex ischemic models. In order to explain the different action of the two compounds, we may hypothesize that they bind to two different parts of the protein which became available based on pH. Specifically, acidic pH drives a conformational change of α-syn that exposes its hydrophobic region which may be the target of Clusterin. At variance, physiological pH keeps a conformation of α-syn that could be targeted by Doxycycline.

Our study has some limitations, such as the use of a mouse model null for α-syn which does not allow us to dissect the specific role of monomeric vs aggregated α-syn in stroke pathophysiology. Thus, our in vivo data needs to be validated in conditional knock out models of α-syn or by using pharmacological means to inhibit the aggregation of the protein at selected time points after stroke. As for our in vitro non-cellular model, the main limitation is represented by the absence of cellular components, not allowing a complete investigation of possible interaction of α-syn with other proteins or cellular components that can influence its aggregation.

In conclusion our study is the first to identify a mechanism of α-syn aggregation in an ischemic environment, which in turn contributes to stroke consequences. The development of toxic aggregated forms of α-syn represent a delayed mechanism following ischemic stroke, which is therefore involved in the secondary mechanisms of stroke lesion expansion. We provide evidence that pathological consequences of aggregated or toxic α-syn involve vascular modifications and resolution of brain edema. As such we propose α-syn aggregation as new pharmacological target to limit secondary damage following ischemic stroke.

REFERENCES

1. GBD 2021 Stroke Risk Factor Collaborators. Global, regional, and national burden of stroke and its risk factors, 1990-2021: a systematic analysis for the Global Burden of Disease Study 2021. *Lancet Neurol.* **23**, 973–1003 (2024).
2. Feigin, V. L. *et al.* World Stroke Organization: Global Stroke Fact Sheet 2025. *Int. J. Stroke* **20**, 132–144 (2025).
3. Hatano, S. Experience from a multicentre stroke register: a preliminary report. *Bull. World Health Organ.* **54**, 541–553 (1976).
4. Rennert, R. C. *et al.* Epidemiology, Natural History, and Clinical Presentation of Large Vessel Ischemic Stroke. *Neurosurgery* **85**, S4–S8 (2019).
5. Brouns, R. & De Deyn, P. P. The complexity of neurobiological processes in acute ischemic stroke. *Clin. Neurol. Neurosurg.* **111**, 483–495 (2009).
6. National Institute of Neurological Disorders and Stroke rt-PA Stroke Study Group. Tissue plasminogen activator for acute ischemic stroke. *N. Engl. J. Med.* **333**, 1581–1587 (1995).
7. Campbell, B. C. V. *et al.* Endovascular therapy for ischemic stroke with perfusion-imaging selection. *N. Engl. J. Med.* **372**, 1009–1018 (2015).
8. Zaidat, O. O. *et al.* Thrombolytic therapy of acute ischemic stroke: correlation of angiographic recanalization with clinical outcome. *AJNR Am. J. Neuroradiol.* **26**, 880–884 (2005).
9. Dorweiler, B. *et al.* Ischemia-Reperfusion Injury: Pathophysiology and Clinical Implications. *Eur. J. Trauma Emerg. Surg. Off. Publ. Eur. Trauma Soc.* **33**, 600–612 (2007).
10. Dirnagl, U., Iadecola, C. & Moskowitz, M. A. Pathobiology of ischaemic stroke: an integrated view. *Trends Neurosci.* **22**, 391–397 (1999).
11. Anrather, J. & Iadecola, C. Inflammation and Stroke: An Overview. *Neurother. J. Am. Soc. Exp. Neurother.* **13**, 661–670 (2016).
12. Fisher, M. & Bastan, B. Identifying and utilizing the ischemic penumbra. *Neurology* **79**, S79-85 (2012).

13. Fagan, S. C., Hess, D. C., Hohnadel, E. J., Pollock, D. M. & Ergul, A. Targets for vascular protection after acute ischemic stroke. *Stroke* **35**, 2220–2225 (2004).

14. Seifert, K. & Heit, J. J. Collateral Blood Flow and Ischemic Core Growth. *Transl. Stroke Res.* **14**, 13–21 (2023).

15. Daneman, R. & Prat, A. The blood-brain barrier. *Cold Spring Harb. Perspect. Biol.* **7**, a020412 (2015).

16. Engelhardt, B. & Sorokin, L. The blood-brain and the blood-cerebrospinal fluid barriers: function and dysfunction. *Semin. Immunopathol.* **31**, 497–511 (2009).

17. Profaci, C. P., Munji, R. N., Pulido, R. S. & Daneman, R. The blood-brain barrier in health and disease: Important unanswered questions. *J. Exp. Med.* **217**, e20190062 (2020).

18. Abbott, N. J., Patabendige, A. A. K., Dolman, D. E. M., Yusof, S. R. & Begley, D. J. Structure and function of the blood-brain barrier. *Neurobiol. Dis.* **37**, 13–25 (2010).

19. Merali, Z., Huang, K., Mikulis, D., Silver, F. & Kassner, A. Evolution of blood-brain-barrier permeability after acute ischemic stroke. *PloS One* **12**, e0171558 (2017).

20. Sarvari, S., Moakedi, F., Hone, E., Simpkins, J. W. & Ren, X. Mechanisms in blood-brain barrier opening and metabolism-challenged cerebrovascular ischemia with emphasis on ischemic stroke. *Metab. Brain Dis.* **35**, 851–868 (2020).

21. Okada, T., Suzuki, H., Travis, Z. D. & Zhang, J. H. The Stroke-Induced Blood-Brain Barrier Disruption: Current Progress of Inspection Technique, Mechanism, and Therapeutic Target. *Curr. Neuropharmacol.* **18**, 1187–1212 (2020).

22. Zhang, W. *et al.* The blood brain barrier in cerebral ischemic injury – Disruption and repair. *Brain Hemorrhages* **1**, 34–53 (2020).

23. Oldendorf, W. H., Cornford, M. E. & Brown, W. J. The large apparent metabolic work capacity of the blood-brain barrier. *Trans. Am. Neurol. Assoc.* **101**, 157–160 (1976).

24. Doll, D. N. *et al.* Mitochondrial crisis in cerebrovascular endothelial cells opens the blood-brain barrier. *Stroke* **46**, 1681–1689 (2015).

25. Kim, Y. *et al.* Effects of Natural Polyphenols on Oxidative Stress-Mediated Blood-Brain Barrier Dysfunction. *Antioxid. Basel Switz.* **11**, 197 (2022).

26. Allen, C. L. & Bayraktutan, U. Oxidative stress and its role in the pathogenesis of ischaemic stroke. *Int. J. Stroke Off. J. Int. Stroke Soc.* **4**, 461–470 (2009).

27. (PDF) Oxidative Stress-Mediated Blood-Brain Barrier (BBB) Disruption in Neurological Diseases. *ResearchGate* (2024) doi:10.1155/2020/4356386.

28. Higashi, Y. *et al.* Endothelial function and oxidative stress in renovascular hypertension. *N. Engl. J. Med.* **346**, 1954–1962 (2002).

29. Nishiyama, A. *et al.* Possible contributions of reactive oxygen species and mitogen-activated protein kinase to renal injury in aldosterone/salt-induced hypertensive rats. *Hypertens. Dallas Tex 1979* **43**, 841–848 (2004).

30. Kim, S.-R. *et al.* Visfatin enhances ICAM-1 and VCAM-1 expression through ROS-dependent NF-kappaB activation in endothelial cells. *Biochim. Biophys. Acta* **1783**, 886–895 (2008).

31. Wang, Q., Tang, X. N. & Yenari, M. A. The inflammatory response in stroke. *J. Neuroimmunol.* **184**, 53–68 (2007).

32. Sato, K. *et al.* Telmisartan reduces progressive oxidative stress and phosphorylated α-synuclein accumulation in stroke-resistant spontaneously hypertensive rats after transient middle cerebral artery occlusion. *J. Stroke Cerebrovasc. Dis. Off. J. Natl. Stroke Assoc.* **23**, 1554–1563 (2014).

33. Fumagalli, S., Perego, C., Pischiutta, F., Zanier, E. R. & De Simoni, M.-G. The ischemic environment drives microglia and macrophage function. *Front. Neurol.* **6**, 81 (2015).

34. Qin, C. *et al.* Dual Functions of Microglia in Ischemic Stroke. *Neurosci. Bull.* **35**, 921–933 (2019).

35. Zhou, W. *et al.* Postischemic brain infiltration of leukocyte subpopulations differs among murine permanent and transient focal cerebral ischemia models. *Brain Pathol. Zurich Switz.* **23**, 34–44 (2013).

36. Chu, H. X. *et al.* Immune cell infiltration in malignant middle cerebral artery infarction: comparison with transient cerebral ischemia. *J. Cereb. Blood Flow Metab. Off. J. Int. Soc. Cereb. Blood Flow Metab.* **34**, 450–459 (2014).

37. Holmes, D. I. R. & Zachary, I. The vascular endothelial growth factor (VEGF) family: angiogenic factors in health and disease. *Genome Biol.* **6**, 209 (2005).

38. Lange, C., Storkebaum, E., de Almodóvar, C. R., Dewerchin, M. & Carmeliet, P. Vascular endothelial growth factor: a neurovascular target in neurological diseases. *Nat. Rev. Neurol.* **12**, 439–454 (2016).

39. Geiseler, S. J. & Morland, C. The Janus Face of VEGF in Stroke. *Int. J. Mol. Sci.* **19**, 1362 (2018).

40. Greenberg, D. A. & Jin, K. Vascular endothelial growth factors (VEGFs) and stroke. *Cell. Mol. Life Sci. CMLS* **70**, 1753–1761 (2013).

41. Bernaudin, M. *et al.* Normobaric hypoxia induces tolerance to focal permanent cerebral ischemia in association with an increased expression of hypoxia-inducible factor-1 and its target genes, erythropoietin and VEGF, in the adult mouse brain. *J. Cereb. Blood Flow Metab. Off. J. Int. Soc. Cereb. Blood Flow Metab.* **22**, 393–403 (2002).

42. Saito, T. *et al.* VEGF-A induces its negative regulator, soluble form of VEGFR-1, by modulating its alternative splicing. *FEBS Lett.* **587**, 2179–2185 (2013).

43. Shibuya, M. Vascular Endothelial Growth Factor (VEGF) and Its Receptor (VEGFR) Signaling in Angiogenesis: A Crucial Target for Anti- and Pro-Angiogenic Therapies. *Genes Cancer* **2**, 1097–1105 (2011).

44. Schoch, H. J., Fischer, S. & Marti, H. H. Hypoxia-induced vascular endothelial growth factor expression causes vascular leakage in the brain. *Brain J. Neurol.* **125**, 2549–2557 (2002).

45. Zhang, H.-T. *et al.* Early VEGF inhibition attenuates blood-brain barrier disruption in ischemic rat brains by regulating the expression of MMPs. *Mol. Med. Rep.* **15**, 57–64 (2017).

46. Yong, V. W., Power, C., Forsyth, P. & Edwards, D. R. Metalloproteinases in biology and pathology of the nervous system. *Nat. Rev. Neurosci.* **2**, 502–511 (2001).

47. Zhao, B.-Q. *et al.* Role of matrix metalloproteinases in delayed cortical responses after stroke. *Nat. Med.* **12**, 441–445 (2006).

48. Arvidsson, A., Collin, T., Kirik, D., Kokaia, Z. & Lindvall, O. Neuronal replacement from endogenous precursors in the adult brain after stroke. *Nat. Med.* **8**, 963–970 (2002).

49. Krupinski, J., Kaluza, J., Kumar, P., Kumar, S. & Wang, J. M. Role of angiogenesis in patients with cerebral ischemic stroke. *Stroke* **25**, 1794–1798 (1994).

50. Beck, H. & Plate, K. H. Angiogenesis after cerebral ischemia. *Acta Neuropathol. (Berl.)* **117**, 481–496 (2009).

51. Zhang, Z. G., Zhang, L., Jiang, Q. & Chopp, M. Bone marrow-derived endothelial progenitor cells participate in cerebral neovascularization after focal cerebral ischemia in the adult mouse. *Circ. Res.* **90**, 284–288 (2002).

52. Custodia, A. *et al.* Unraveling the potential of endothelial progenitor cells as a treatment following ischemic stroke. *Front. Neurol.* **13**, 940682 (2022).

53. Gandin, C., Widmann, C., Lazdunski, M. & Heurteaux, C. MLC901 Favors Angiogenesis and Associated Recovery after Ischemic Stroke in Mice. *Cerebrovasc. Dis. Basel Switz.* **42**, 139–154 (2016).

54. Kanazawa, M. *et al.* Microglia preconditioned by oxygen-glucose deprivation promote functional recovery in ischemic rats. *Sci. Rep.* **7**, 42582 (2017).

55. Wang, Z. *et al.* Chronic valproate treatment enhances postischemic angiogenesis and promotes functional recovery in a rat model of ischemic stroke. *Stroke* **43**, 2430–2436 (2012).

56. Goedert, M. Alpha-synuclein and neurodegenerative diseases. *Nat. Rev. Neurosci.* **2**, 492–501 (2001).

57. Villar-Piqué, A., Lopes da Fonseca, T. & Outeiro, T. F. Structure, function and toxicity of alpha-synuclein: the Bermuda triangle in synucleinopathies. *J. Neurochem.* **139 Suppl 1**, 240–255 (2016).

58. Pei, Y. & Maitta, R. W. Alpha synuclein in hematopoiesis and immunity. *Heliyon* **5**, e02590 (2019).

59. Fukuda, I. Expression of α-synuclein in vascular endothelial and smooth muscle cells. *Int. Congr. Ser.* (2003).

60. Tamo, W. *et al.* Expression of alpha-synuclein, the precursor of non-amyloid beta component of Alzheimer's disease amyloid, in human cerebral blood vessels. *Neurosci. Lett.* **326**, 5–8 (2002).

61. Calo, L., Wegrzynowicz, M., Santivañez-Perez, J. & Grazia Spillantini, M. Synaptic failure and α-synuclein. *Mov. Disord. Off. J. Mov. Disord. Soc.* **31**, 169–177 (2016).

62. Bellucci, A. *et al.* From α-synuclein to synaptic dysfunctions: new insights into the pathophysiology of Parkinson's disease. *Brain Res.* **1476**, 183–202 (2012).

63. Faustini, G. *et al.* Alpha-Synuclein Preserves Mitochondrial Fusion and Function in Neuronal Cells. *Oxid. Med. Cell. Longev.* **2019**, 4246350 (2019).

64. Longhena, F., Faustini, G., Spillantini, M. G. & Bellucci, A. Living in Promiscuity: The Multiple Partners of Alpha-Synuclein at the Synapse in Physiology and Pathology. *Int. J. Mol. Sci.* **20**, 141 (2019).

65. Giasson, B. I., Murray, I. V., Trojanowski, J. Q. & Lee, V. M. A hydrophobic stretch of 12 amino acid residues in the middle of alpha-synuclein is essential for filament assembly. *J. Biol. Chem.* **276**, 2380–2386 (2001).

66. Dedmon, M. M., Lindorff-Larsen, K., Christodoulou, J., Vendruscolo, M. & Dobson, C. M. Mapping long-range interactions in alpha-synuclein using spin-label NMR and ensemble molecular dynamics simulations. *J. Am. Chem. Soc.* **127**, 476–477 (2005).

67. Conway, K. A., Harper, J. D. & Lansbury, P. T. Accelerated in vitro fibril formation by a mutant alpha-synuclein linked to early-onset Parkinson disease. *Nat. Med.* **4**, 1318–1320 (1998).

68. Gurry, T. *et al.* The dynamic structure of α-synuclein multimers. *J. Am. Chem. Soc.* **135**, 3865–3872 (2013).

69. Peelaerts, W. & Baekelandt, V. α-Synuclein strains and the variable pathologies of synucleinopathies. *J. Neurochem.* **139 Suppl 1**, 256–274 (2016).

70. Cheng, F., Vivacqua, G. & Yu, S. The role of α-synuclein in neurotransmission and synaptic plasticity. *J. Chem. Neuroanat.* **42**, 242–248 (2011).

71. Guardia-Laguarta, C., Area-Gomez, E., Schon, E. A. & Przedborski, S. Novel subcellular localization for α-synuclein: possible functional consequences. *Front. Neuroanat.* **9**, 17 (2015).

72. Maroteaux, L., Campanelli, J. T. & Scheller, R. H. Synuclein: a neuron-specific protein localized to the nucleus and presynaptic nerve terminal. *J. Neurosci. Off. J. Soc. Neurosci.* **8**, 2804–2815 (1988).

73. Pinho, R. *et al.* Nuclear localization and phosphorylation modulate pathological effects of alpha-synuclein. *Hum. Mol. Genet.* **28**, 31–50 (2019).

74. Li, W.-W. *et al.* Localization of alpha-synuclein to mitochondria within midbrain of mice. *Neuroreport* **18**, 1543–1546 (2007).

75. Siddiqui, A. *et al.* Selective binding of nuclear alpha-synuclein to the PGC1alpha promoter under conditions of oxidative stress may contribute to losses in mitochondrial function: implications for Parkinson's disease. *Free Radic. Biol. Med.* **53**, 993–1003 (2012).

76. Parihar, M. S., Parihar, A., Fujita, M., Hashimoto, M. & Ghafourifar, P. Mitochondrial association of alpha-synuclein causes oxidative stress. *Cell. Mol. Life Sci. CMLS* **65**, 1272–1284 (2008).

77. Garcia-Reitboeck, P. *et al.* Endogenous alpha-synuclein influences the number of dopaminergic neurons in mouse substantia nigra. *Exp. Neurol.* **248**, 541–545 (2013).

78. Spillantini, M. G., Crowther, R. A., Jakes, R., Hasegawa, M. & Goedert, M. alpha-Synuclein in filamentous inclusions of Lewy bodies from Parkinson's disease and dementia with lewy bodies. *Proc. Natl. Acad. Sci. U. S. A.* **95**, 6469–6473 (1998).

79. Braak, H. *et al.* Staging of brain pathology related to sporadic Parkinson's disease. *Neurobiol. Aging* **24**, 197–211 (2003).

80. Engelender, S. & Isacson, O. The Threshold Theory for Parkinson's Disease. *Trends Neurosci.* **40**, 4–14 (2017).

81. El-Agnaf, O. M. A. *et al.* Alpha-synuclein implicated in Parkinson's disease is present in extracellular biological fluids, including human plasma. *FASEB J. Off. Publ. Fed. Am. Soc. Exp. Biol.* **17**, 1945–1947 (2003).

82. Danzer, K. M. *et al.* Heat-shock protein 70 modulates toxic extracellular α-synuclein oligomers and rescues trans-synaptic toxicity. *FASEB J. Off. Publ. Fed. Am. Soc. Exp. Biol.* **25**, 326–336 (2011).

83. Lee, H.-J., Shin, S. Y., Choi, C., Lee, Y. H. & Lee, S.-J. Formation and removal of alpha-synuclein aggregates in cells exposed to mitochondrial inhibitors. *J. Biol. Chem.* **277**, 5411–5417 (2002).

84. Jang, A. *et al.* Non-classical exocytosis of alpha-synuclein is sensitive to folding states and promoted under stress conditions. *J. Neurochem.* **113**, 1263–1274 (2010).

85. Sui, Y.-T., Bullock, K. M., Erickson, M. A., Zhang, J. & Banks, W. A. Alpha synuclein is transported into and out of the brain by the blood-brain barrier. *Peptides* **62**, 197–202 (2014).

86. Dieriks, B. V. *et al.* α-synuclein transfer through tunneling nanotubes occurs in SH-SY5Y cells and primary brain pericytes from Parkinson's disease patients. *Sci. Rep.* **7**, 42984 (2017).

87. Peng, C., Trojanowski, J. Q. & Lee, V. M.-Y. Protein transmission in neurodegenerative disease. *Nat. Rev. Neurol.* **16**, 199–212 (2020).

88. Zou, W. *et al.* Blocking meningeal lymphatic drainage aggravates Parkinson's disease-like pathology in mice overexpressing mutated α-synuclein. *Transl. Neurodegener.* **8**, 7 (2019).

89. Kim, T. *et al.* Poststroke Induction of α-Synuclein Mediates Ischemic Brain Damage. *J. Neurosci. Off. J. Soc. Neurosci.* **36**, 7055–7065 (2016).

90. Unal-Cevik, I. *et al.* Alpha-synuclein aggregation induced by brief ischemia negatively impacts neuronal survival in vivo: a study in [A30P]alpha-synuclein transgenic mouse. *J. Cereb. Blood Flow Metab. Off. J. Int. Soc. Cereb. Blood Flow Metab.* **31**, 913–923 (2011).

91. Wu, Z. *et al.* Alpha-synuclein alterations in red blood cells of peripheral blood after acute ischemic stroke. *Int. J. Clin. Exp. Pathol.* **12**, 1757–1763 (2019).

92. Zhao, H.-Q., Li, F.-F., Wang, Z., Wang, X.-M. & Feng, T. A comparative study of the amount of α-synuclein in ischemic stroke and Parkinson's disease. *Neurol. Sci. Off. J. Ital. Neurol. Soc. Ital. Soc. Clin. Neurophysiol.* **37**, 749–754 (2016).

93. Koh, P.-O. Cerebral ischemic injury decreases α-synuclein expression in brain tissue and glutamate-exposed HT22 cells. *Lab. Anim. Res.* **33**, 244–250 (2017).

94. Kim, T. *et al.* The microRNA miR-7a-5p ameliorates ischemic brain damage by repressing α-synuclein. *Sci. Signal.* **11**, eaat4285 (2018).

95. Junn, E. *et al.* Repression of alpha-synuclein expression and toxicity by microRNA-7. *Proc. Natl. Acad. Sci. U. S. A.* **106**, 13052–13057 (2009).

96. Matsumoto, J. *et al.* Transmission of α-synuclein-containing erythrocyte-derived extracellular vesicles across the blood-brain barrier via adsorptive mediated transcytosis: another mechanism for initiation and progression of Parkinson's disease? *Acta Neuropathol. Commun.* **5**, 71 (2017).

97. Ishimaru, H., Uéda, K., Takahashi, A. & Maruyama, Y. Changes in presynaptic protein NACP/alpha-synuclein in an ischemic gerbil hippocampus. *Brain Res.* **788**, 311–314 (1998).

98. Aird, W. C. Phenotypic heterogeneity of the endothelium: I. Structure, function, and mechanisms. *Circ. Res.* **100**, 158–173 (2007).

99. Florey. The endothelial cell. *Br. Med. J.* **2**, 487–490 (1966).

100. Liebner, S. *et al.* Functional morphology of the blood-brain barrier in health and disease. *Acta Neuropathol. (Berl.)* **135**, 311–336 (2018).

101. Lapenna, A., De Palma, M. & Lewis, C. E. Author Correction: Perivascular macrophages in health and disease. *Nat. Rev. Immunol.* **21**, 752 (2021).

102. Bogale, T. A. *et al.* Alpha-Synuclein in the Regulation of Brain Endothelial and Perivascular Cells: Gaps and Future Perspectives. *Front. Immunol.* **12**, 611761 (2021).

103. Kuan, W.-L. *et al.* α-Synuclein pre-formed fibrils impair tight junction protein expression without affecting cerebral endothelial cell function. *Exp. Neurol.* **285**, 72–81 (2016).

104. Kim, K. S., Park, J.-Y., Jou, I. & Park, S. M. Regulation of Weibel-Palade body exocytosis by alpha-synuclein in endothelial cells. *J. Biol. Chem.* **285**, 21416–21425 (2010).

105. Takami, Y. *et al.* Novel pathophysiological roles of α-synuclein in age-related vascular endothelial dysfunction. *FASEB J. Off. Publ. Fed. Am. Soc. Exp. Biol.* **36**, e22555 (2022).

106. Lowenstein, C. J., Morrell, C. N. & Yamakuchi, M. Regulation of Weibel-Palade body exocytosis. *Trends Cardiovasc. Med.* **15**, 302–308 (2005).

107. Petri, B. *et al.* von Willebrand factor promotes leukocyte extravasation. *Blood* **116**, 4712–4719 (2010).

108. Nagatsu, T., Mogi, M., Ichinose, H. & Togari, A. Cytokines in Parkinson's disease. *J. Neural Transm. Suppl.* 143–151 (2000).

109. Pober, J. S. & Sessa, W. C. Evolving functions of endothelial cells in inflammation. *Nat. Rev. Immunol.* **7**, 803–815 (2007).

110. Pediaditakis, I. *et al.* Modeling alpha-synuclein pathology in a human brain-chip to assess blood-brain barrier disruption. *Nat. Commun.* **12**, 5907 (2021).

111. Guan, J. *et al.* Vascular degeneration in Parkinson's disease. *Brain Pathol. Zurich Switz.* **23**, 154–164 (2013).

112. Desai Bradaric, B., Patel, A., Schneider, J. A., Carvey, P. M. & Hendey, B. Evidence for angiogenesis in Parkinson's disease, incidental Lewy body disease, and progressive supranuclear palsy. *J. Neural Transm. Vienna Austria 1996* **119**, 59–71 (2012).

113. Gray, M. T. & Woulfe, J. M. Striatal blood-brain barrier permeability in Parkinson's disease. *J. Cereb. Blood Flow Metab. Off. J. Int. Soc. Cereb. Blood Flow Metab.* **35**, 747–750 (2015).

114. Elabi, O. *et al.* Human α-synuclein overexpression in a mouse model of Parkinson's disease leads to vascular pathology, blood brain barrier leakage and pericyte activation. *Sci. Rep.* **11**, 1120 (2021).

115. Dieriks, B. V. *et al.* Human pericytes degrade diverse α-synuclein aggregates. *PloS One* **17**, e0277658 (2022).

116. Tj, S. *et al.* Pericytes take up and degrade α-synuclein but succumb to apoptosis under cellular stress. *Sci. Rep.* **12**, (2022).

117. Dohgu, S. *et al.* Monomeric α-synuclein induces blood-brain barrier dysfunction through activated brain pericytes releasing inflammatory mediators in vitro. *Microvasc. Res.* **124**, 61–66 (2019).

118. Galkin, M., Priss, A., Kyriukha, Y. & Shvadchak, V. Navigating α-Synuclein Aggregation Inhibition: Methods, Mechanisms, and Molecular Targets. *Chem. Rec. N. Y. N* **24**, e202300282 (2024).

119. Charnay, Y. *et al.* Clusterin in neurological disorders: molecular perspectives and clinical relevance. *Brain Res. Bull.* **88**, 434–443 (2012).

120. Lidström, A.-M. *et al.* Normal levels of clusterin in cerebrospinal fluid in Alzheimer's disease, and no change after acute ischemic stroke. *J. Alzheimers Dis. JAD* **3**, 435–442 (2001).

121. Lenzi, C. *et al.* The Down-Regulation of Clusterin Expression Enhances the αSynuclein Aggregation Process. *Int. J. Mol. Sci.* **21**, 7181 (2020).

122. Reglodi, D. *et al.* Novel tactics for neuroprotection in Parkinson's disease: Role of antibiotics, polyphenols and neuropeptides. *Prog. Neurobiol.* **155**, 120–148 (2017).

123. Cho, Y. *et al.* Doxycycline is neuroprotective against nigral dopaminergic degeneration by a dual mechanism involving MMP-3. *Neurotox. Res.* **16**, 361–371 (2009).

124. Lazzarini, M. *et al.* Doxycycline restrains glia and confers neuroprotection in a 6-OHDA Parkinson model. *Glia* **61**, 1084–1100 (2013).

125. Dominguez-Meijide, A. *et al.* Doxycycline inhibits α-synuclein-associated pathologies in vitro and in vivo. *Neurobiol. Dis.* **151**, 105256 (2021).

126. Pires, P. W. *et al.* Doxycycline, a matrix metalloprotease inhibitor, reduces vascular remodeling and damage after cerebral ischemia in stroke-prone spontaneously hypertensive rats. *Am. J. Physiol. - Heart Circ. Physiol.* **301**, H87–H97 (2011).

127. Percie du Sert, N. *et al.* The IMPROVE Guidelines (Ischaemia Models: Procedural Refinements Of in Vivo Experiments). *J. Cereb. Blood Flow Metab. Off. J. Int. Soc. Cereb. Blood Flow Metab.* **37**, 3488–3517 (2017).

128. Valente, A. *et al.* Harmonization of sensorimotor deficit assessment in a registered multicentre pre-clinical randomized controlled trial using two models of ischemic stroke. *J. Cereb. Blood Flow Metab. Off. J. Int. Soc. Cereb. Blood Flow Metab.* **43**, 1077–1088 (2023).

129. Mercurio, D. *et al.* Inhibition of mannan-binding lectin associated serine protease (MASP)-2 reduces the cognitive deficits in a mouse model of severe traumatic brain injury. *J. Neuroinflammation* **21**, 141 (2024).

130. Meisl, G. *et al.* Molecular mechanisms of protein aggregation from global fitting of kinetic models. *Nat. Protoc.* **11**, 252–272 (2016).

131. Mercurio, D. *et al.* Plasma-derived and recombinant C1 esterase inhibitor: Binding profiles and neuroprotective properties in brain ischemia/reperfusion injury. *Brain. Behav. Immun.* **93**, 299–311 (2021).

132. Dominguez-Meijide, A. *et al.* Doxycycline inhibits α-synuclein-associated pathologies *in vitro* and *in vivo*. *Neurobiol. Dis.* **151**, 105256 (2021).

133. Beeg, M. *et al.* Clusterin Binds to Aβ1–42 Oligomers with High Affinity and Interferes with Peptide Aggregation by Inhibiting Primary and Secondary Nucleation*. *J. Biol. Chem.* **291**, 6958–6966 (2016).

134. Zha, X., Xiong, Z.-G. & Simon, R. P. pH and proton-sensitive receptors in brain ischemia. *J. Cereb. Blood Flow Metab.* **42**, 1349–1363 (2022).